Bendix

Aerospace Systems Division

ALSEP Fuel Cask and Support Structure Prototype (D-1) Vibration Test Evaluation

DATE 8/5/68

This memorandum presents the evaluation of the data obtained from the prototype ALSEP cask assembly vibration test conducted in April 1968.

Prepared by: J. Maszatics
J. Maszatics

Approved by: M. Katz
M. Katz

CONTENTS

LIST OF FIGURES

1.0 SUMMARY

The prototype ALSEP cask assembly was subjected to a series of qualification level launch and boost vibration tests. No structural failures occurred. The random response was considerably less than predicted by analysis and the sinusoidal response was somewhat higher than predicted.

2.0 REFERENCES

2.1 ALSEP Fuel Cask Mount Proto A Vibration, TR 3101, Systems Test Dept., Bendix Aerospace Systems Div., 21 June 1968.

2.2 Results of the Three Dimensional Dynamic Analysis on the ALSEP Cask and Mounting Structure Unit, Letter No. 1098-0113, Bendix Research Laboratories, 19 March 1968.

3.0 TEST DESCRIPTION

The ALSEP RTG fuel cask and support structure (commonly referred to as the ALSEP Cask Assembly and abbreviated ACA) prototype D-1 was subjected to a series of vibration tests at the Bendix Mishawaka Division from 11 April 1968 to 13 April 1968. The following tests were conducted in each orthogonal axis as defined in figure 1.

(a) transmissibility survey (1g sinusoidal sweep) from 5 to 2000 cps at launch and boost flight phase temperature (280 F)

(b) transmissibility survey (1g sinusoidal sweep) from 5 to 2000 cps at lunar descent flight phase temperature (600 F)

(c) launch and boost phase sinusoidal vibration (figure 2)

(d) launch and boost phase random vibration (figure 3)

Accelerometers were located as shown in figure 1. Their purpose was to record the vibration environment at the interface of the Bendix support structure and the GE cask.

A full description of the test, including procedure and data is given in ref. 2.1.

4.0 TEST RESULTS

The complete set of vibration data (T-plots, peak g-plots, and PSD plots) can be found in reference 2.1.

The data obtained at the five locations shown in figure 1 exhibited no substantial differences from one location to another.

No structural failures were observed.

4.1 Recommended Cask Vibration Specification

Figures 6 through 14 show the cask vibration specifications determined as described below from test data.

4.1.1 Launch and Boost Sinusoidal Specification

The X-axis sine specification was established by enveloping all of the X response data (locations 1 through 5 and X, Y, and Z input) with a constant peak-g line and a constant double amplitude line with a cross-over point between 15 and 30 cps. Similarly for the Y and Z axes specifications. The results are shown in figures 6, 7 and 8.

4.1.2 Launch and Boost Random Specification

The X-axis random specification was established by enveloping all of the X response data (locations 1 through 5 and X, Y, and Z input) with constant g^2/cps lines and constant db/octave lines. Since the response levels were at many frequencies less than the input level, the additional restriction was imposed that the cask specification be equal to or greater than the input specification at all frequencies. The results of this procedure are shown in figures 9, 10 and 11 for the X, Y, and Z axes respectively.

4.1.3 Lunar Descent Sinusoidal Specification

Because the lunar descent input levels are considerably less severe than those for launch and boost (compare figures 2 and 3 with figures 4 and 5), the lunar descent sine and random tests were not conducted on the prototype. However due to the temperature difference between the two phases of flight, it was considered worthwhile for purposes of comparison to run a 1g sinusoidal transmissibility survey from 5 to 2000 cps at the lunar descent temperature (see section 4. 5).

The sinusoidal response data was calculated using the transmissibility data from the 1g sweeps. That is, output equals input times transmissibility at a given frequency. Typical transmissibility plots are shown in figures 22, 23, and 24. The sinusoidal input is given in figure 4.

The lunar descent sinusoidal specification for the cask was determined by enveloping the response data, regardless of output direction or accelerometer location, using a constant peak-g line and a constant double amplitude line with a cross-over point between 15 and 30 cps. In this way one specification curve (shown in figure 12) was established for all three directions. The low levels did not warrant distinguishing between axes.

4. 1. 4 Lunar Descent Random Specification

As with the sinusoidal data, lunar descent random response data was not available and therefore had to be calculated. The theoretical formula is, output equals input times the square of the transmissibility at a given frequency. Since the above formula assumes damping to be independent of input level, the calculated response data is only an approximation. Hence the random specifications determined from such data should not necessarily envelope all of the data. The specifications, shown in figures 13 and 14, are based upon the calculated response data which was modified with consideration given to the response data obtained from the launch and boost random tests.

4. 2 Comparison With Analysis

Figures 15, 16 and 17 show transmissibility functions from analysis (ref. 2. 2) and test (1g sweep) for the x, y, and z axes respectively. The analysis considered four cases which arose from two parameters: (1) hinged and fixed end supports between trunnions and cask and (2) percentage of critical damping (5% and 10% were used).

The analysis data shown represents hinged end supports and 10% damping. The correlation with test results is fairly good for transmissibility, but the calculated random and full level sinusoidal response does not correlate at all with test results. This will be discussed in section 4. 5.

4.3 Cross-Axis Motion

As would be expected from the cantilever type structure shown in figure 1, there was a high degree of cross-axis motion present during all the vibration tests. Figure 18 shows one of the more severe examples. For a 1g sinusoidal input in the X-axis from 5 to 2000 cps, the response in the Z-axis shows a transmissibility grater than unity at many frequencies. The maximum occurred at 44 cps with a value of 2.1. This data was obtained at location 5 on the cask (see figure 1).

4.4 Temperature Effects

Although the lunar descent phase vibration environment is much less severe than the launch and boost phase, there is a significant temperature difference. In order to investigate the effects of temperature upon the dynamic characteristics of the system, a transmissibility survey was taken in each coordinate axis at the lunar descent temperature (600°F).

By comparing the data thus obtained with the corresponding data gathered from transmissibility surveys at launch and boost temperature (280°F), the following trends were noted.

(a) For X-response to X-input the first mode transmissibility was higher at the higher temperature. Figures 19 (launch & boost) and 22 (lunar descent) are typical. The first mode transmissibility increased from 2.5 to 3.4 when the temperature was increased from 280°F to 600°F.

(b) For Y-response to Y-input the first mode transmissibility increased slightly with temperature. Figures 20 and 23, which are typical, show an increase from 3.8 at 280°F to 4.2 at 600°F.

(c) For Z-response to Z-input the first mode transmissibility did not change significantly with temperature. However, the first mode transmissibility was not the highest as it was for the other two axes. At a later mode the maximum transmissibility was reduced by an increase in temperature. Figures 21 and 24 are typical where the maximum transmissibility was 5.6 at 280°F and was decreased to 4.2

at 600°F. A curious trend was noticed at 280 cps. At the launch and boost temperature it was an antiresonant frequency, but at the lunar descent temperature it was a resonant frequency.

4.5 Non-Linear Damping

Generally, the factors that determine the degree of damping within a structure are dependent upon the level of dynamic loading. It would therefore be expected that transmissibilities would show a certain amount of variation between the 1g surveys and the full level sinusoidal tests.

Figures 25, 26 and 27 show typical transmissibility functions obtained from the launch and boost sinusoidal vibration tests for X-response to X-input, Y-response to Y-input, and Z-response to Z-input respectively. In the X-axis the first mode transmissibility increased from 3.3 to 3.8. In the Y-axis the transmissibility increased from 4.0 to 6.9 and the natural frequency shifted from 31 to 40 cps. There were no significant changes noted in the Z-axis for frequencies below 100 cps (the full level sinusoidal tests do not exceed 100 cps).

The combination of structural members which make up the ALSEP cask assembly have an inherent damping mechanism which is not capable of absorbing energy beyond a certain limit. Hence, as the energy put into the system is increased beyond the limit the resulting transmissibility increases. This seems to be true for the X-axis and especially the Y-axis.

5.0 CONCLUSIONS

The transmissibilities obtained from the 1g sweep surveys were in fair agreement with predicted values determined by analysis. However, due to non-linear damping effects the response to full level sinusoidal and random vibration were significantly different from predicted values. The random response levels were significantly less than predicted levels (about an order of magnitude less), while the sinusoidal response level in the Y-axis was about 50% higher than predicted.

Comparing data obtained at location 4 on the trunnion with location 5 on the cask indicates that the difference in transmissibility between these points is negligible.

Comparing 1g sweep transmissibility data at 600°F and 280°F shows that the temperature difference between launch and boost conditions and lunar descent conditions does affect the system dynamic characteristics, but not significantly.

ACCELEROMETER LOCATIONS

1 Response Accelerometer in direction of vibration
4 Response Accelerometer in direction of vibration
5 Triaxial Response Accelerometer
6 Triaxial Response Accelerometer

NOTE: Location 2 and 3 will be used if the accelerometer blocks at locations 5 and 6 come off during vibration.

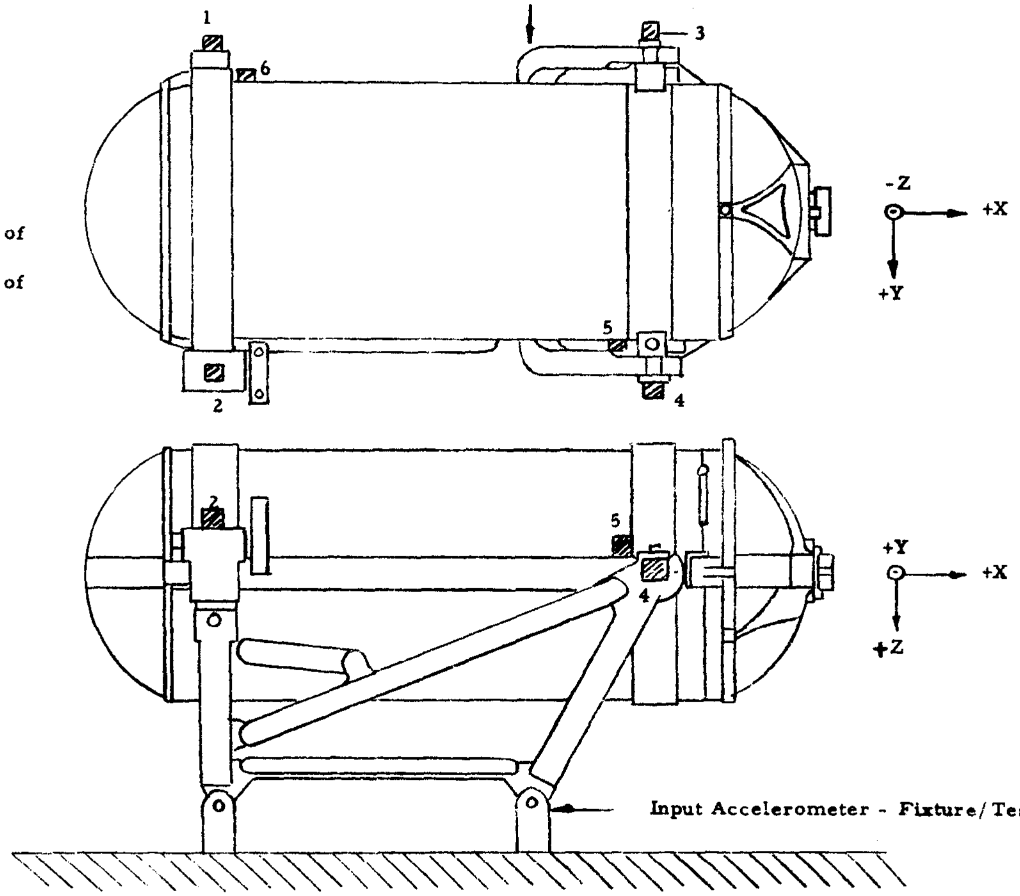

VIBRATION TEST SETUP

FIG. 1

RTG FUEL CASK & SUPPORT STRUCTURE
X, Y, Z AXES
LAUNCH & BOOST
SINUSOIDAL VIBRATION SPECIFICATION

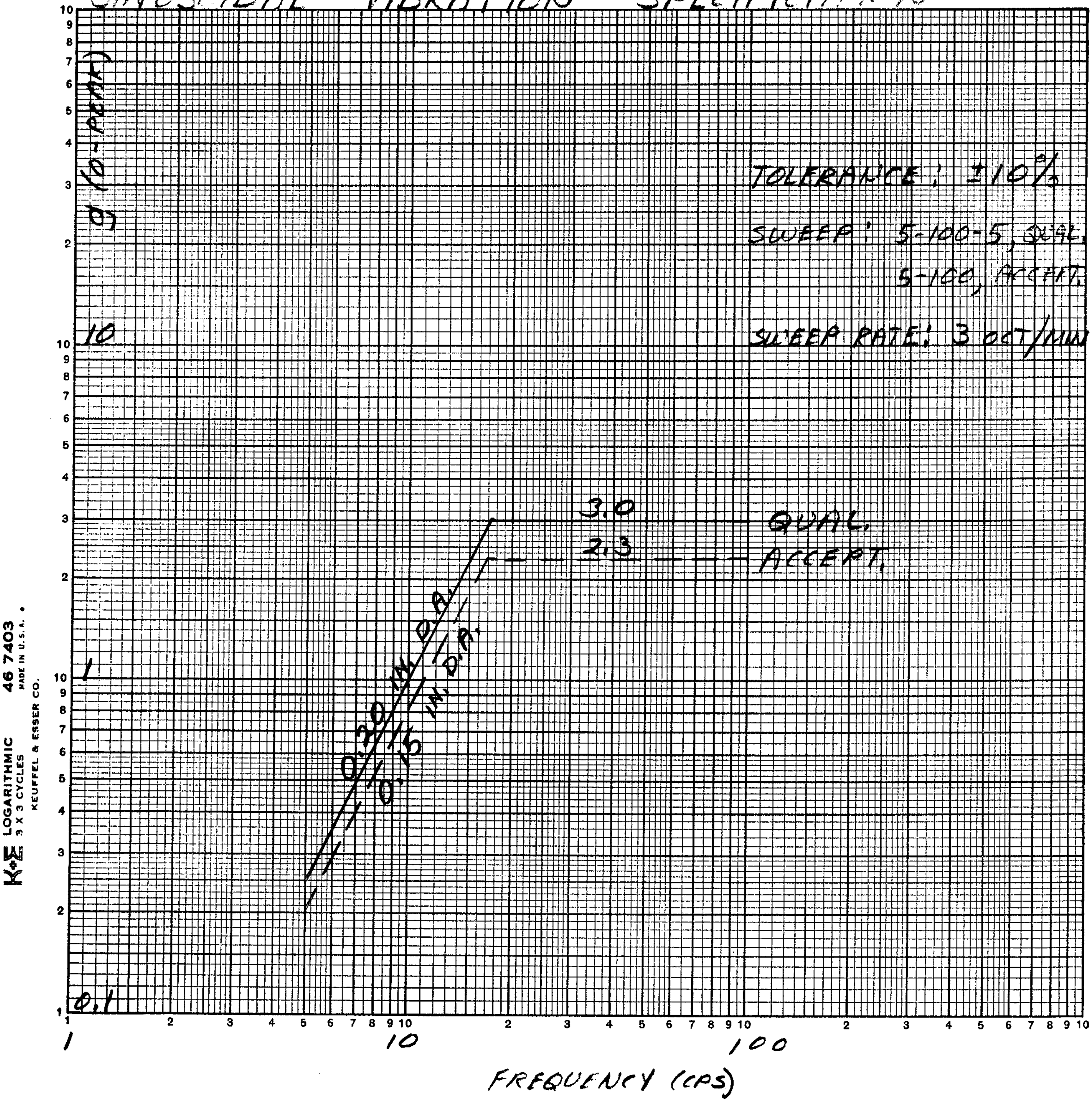

FIG. 2

RTG FUEL CASK & SUPPORT STRUCTURE
X, Y, Z AXES
LAUNCH & BOOST
RANDOM VIBRATION SPECIFICATION

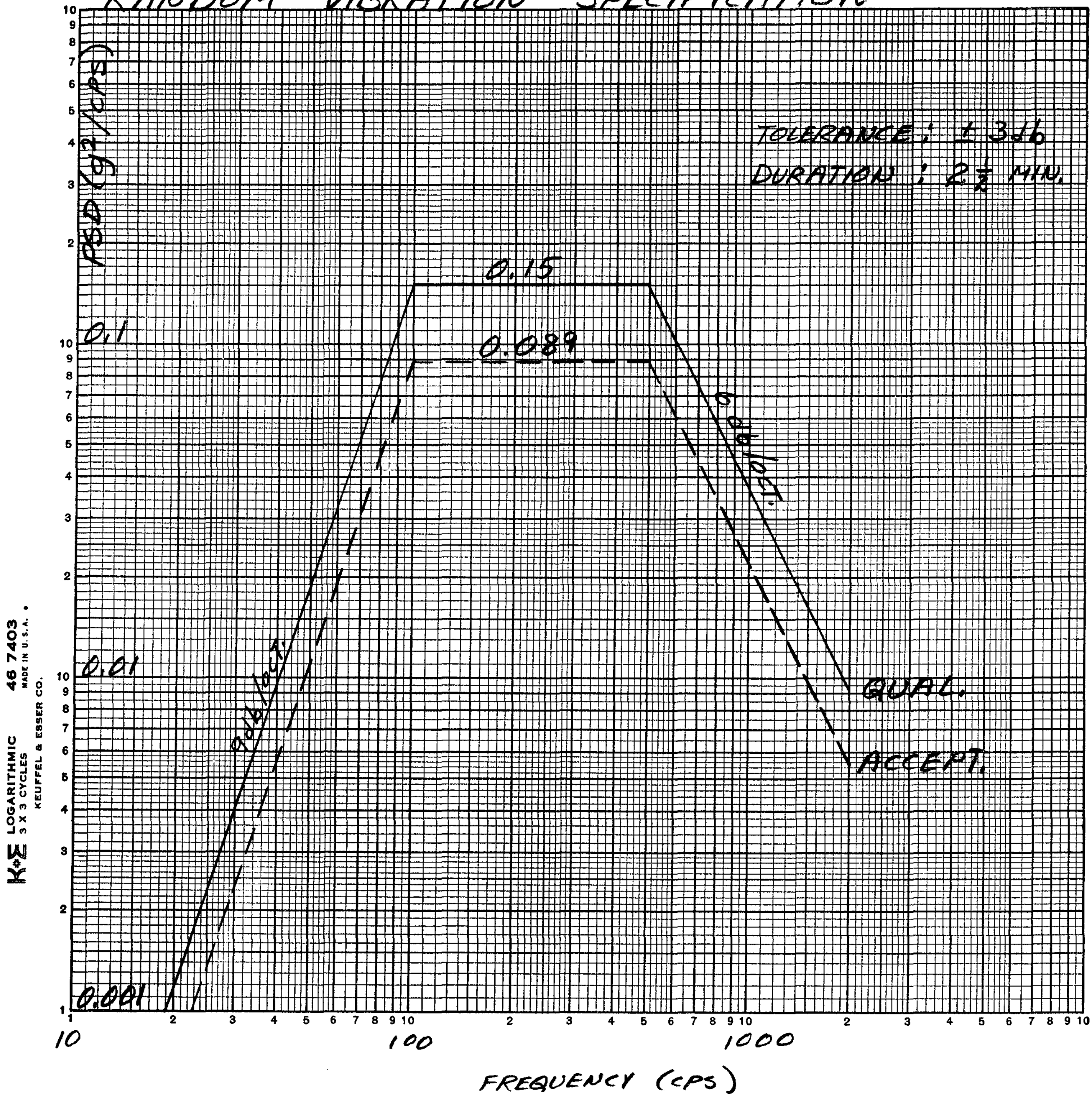

FIG. 3

RTG FUEL CASK & SUPPORT STRUCTURE
X, Y, Z AXES
LUNAR DESCENT
SINUSOIDAL VIBRATION SPECIFICATION

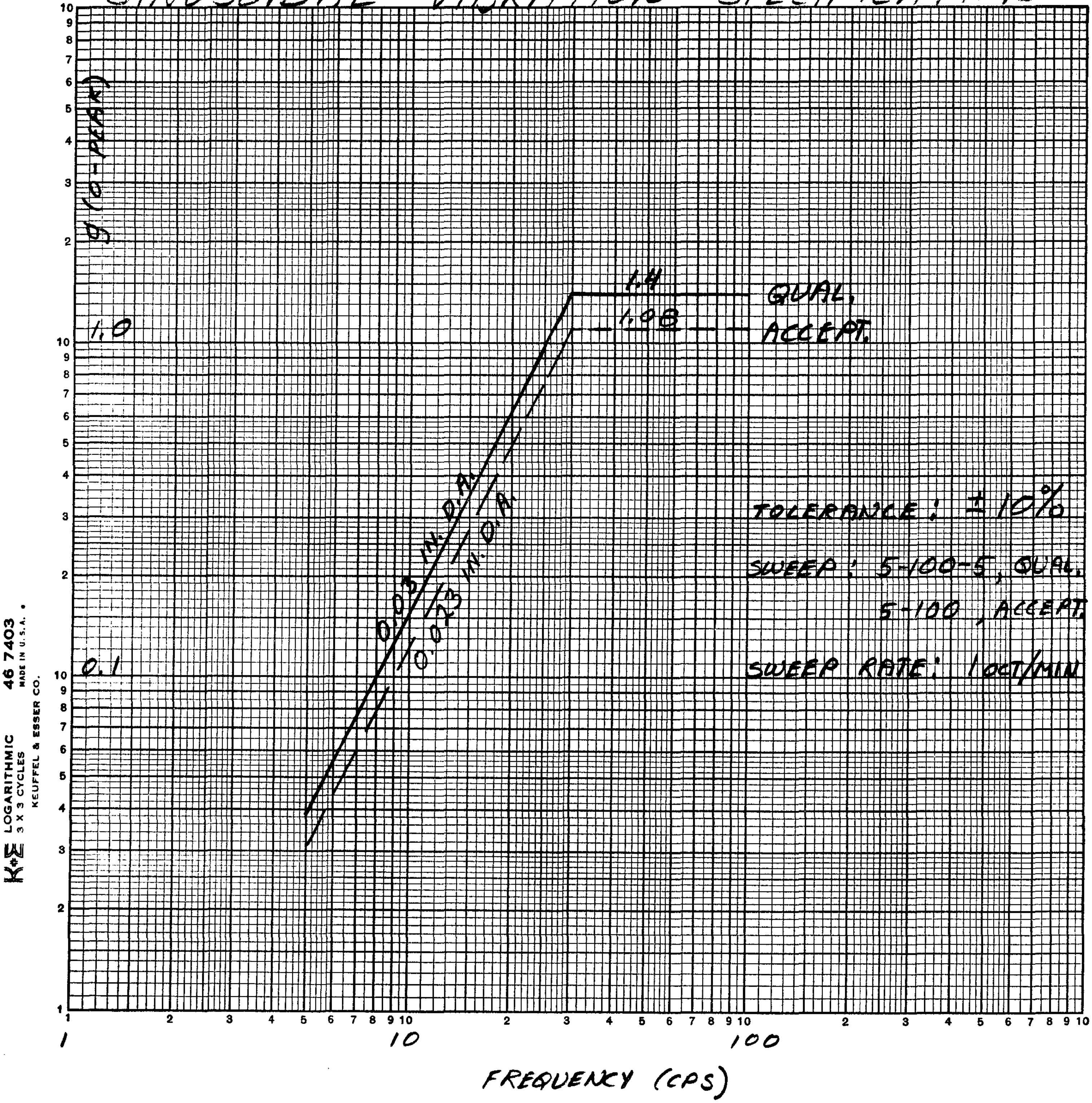

FIG. 4

RTG FUEL CASK & SUPPORT STRUCTURE
X, Y, Z AXES
LUNAR DESCENT
RANDOM VIBRATION SPECIFICATION

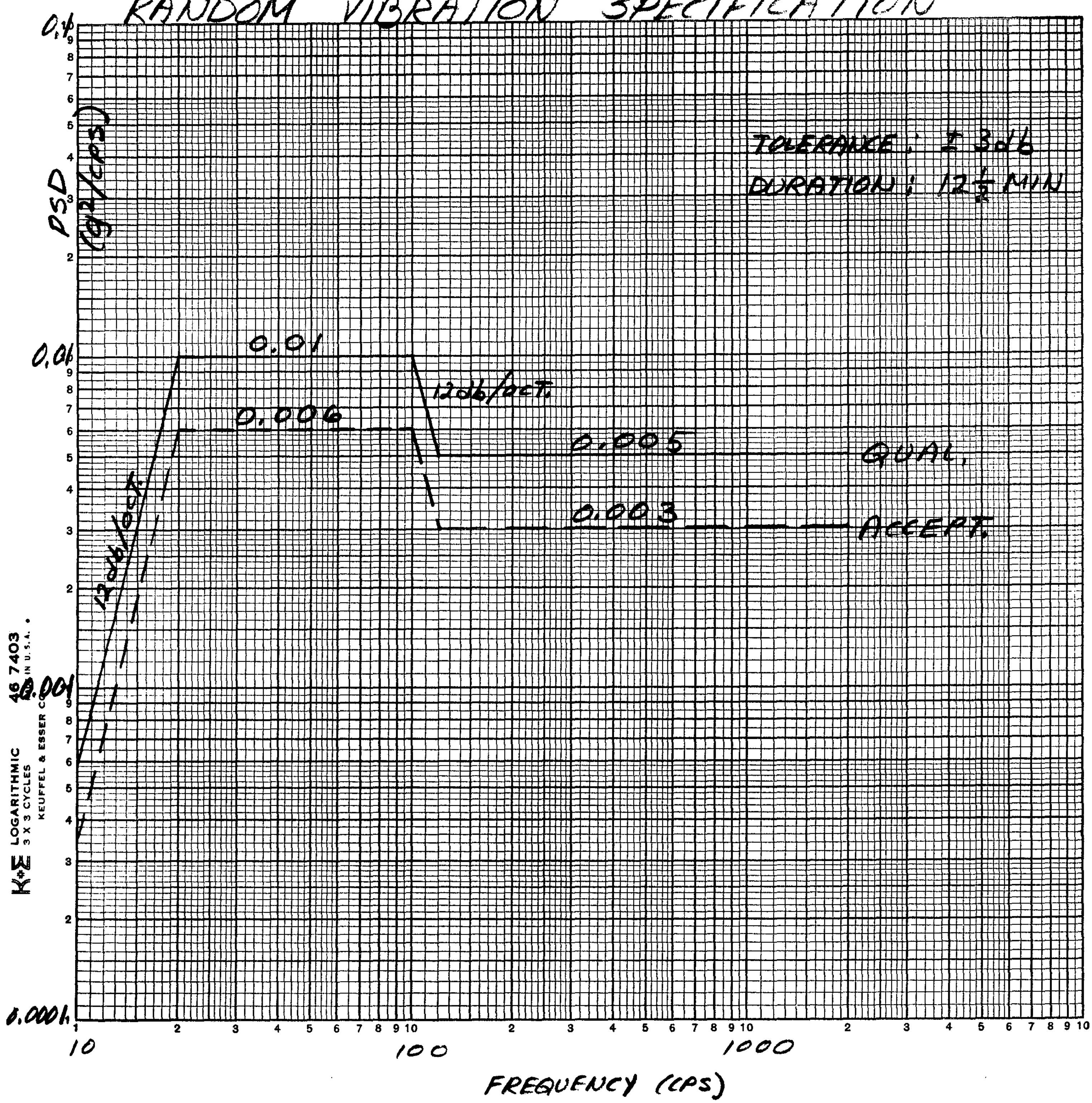

FIG. 5

RTG FUEL CASK
X - AXIS
LAUNCH & BOOST
SINUSOIDAL VIBRATION SPECIFICATION

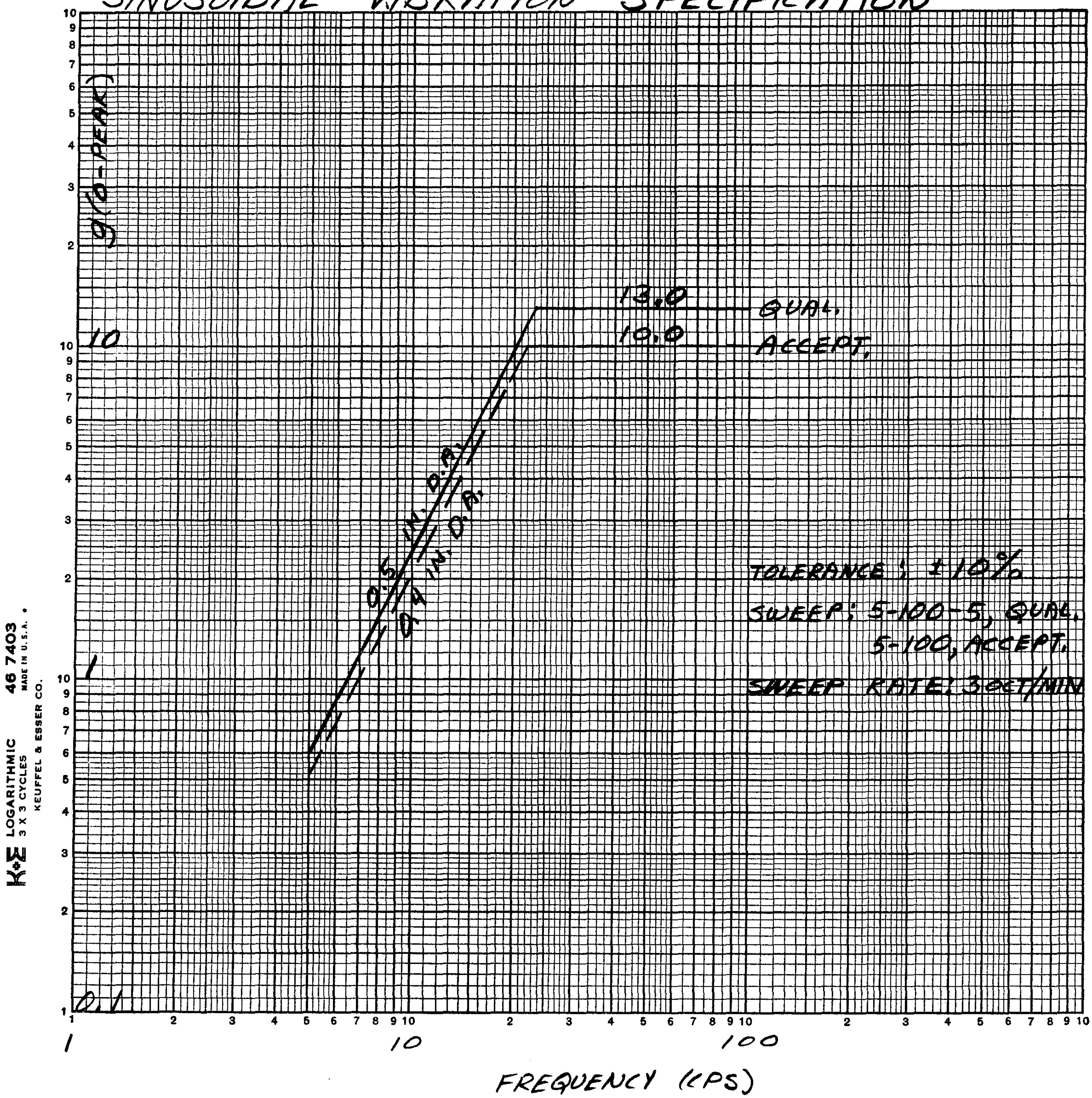

FIG. 6

RTG FUEL CASK
Y-AXIS
LAUNCH & BOOST
SINUSOIDAL VIBRATION SPECIFICATION

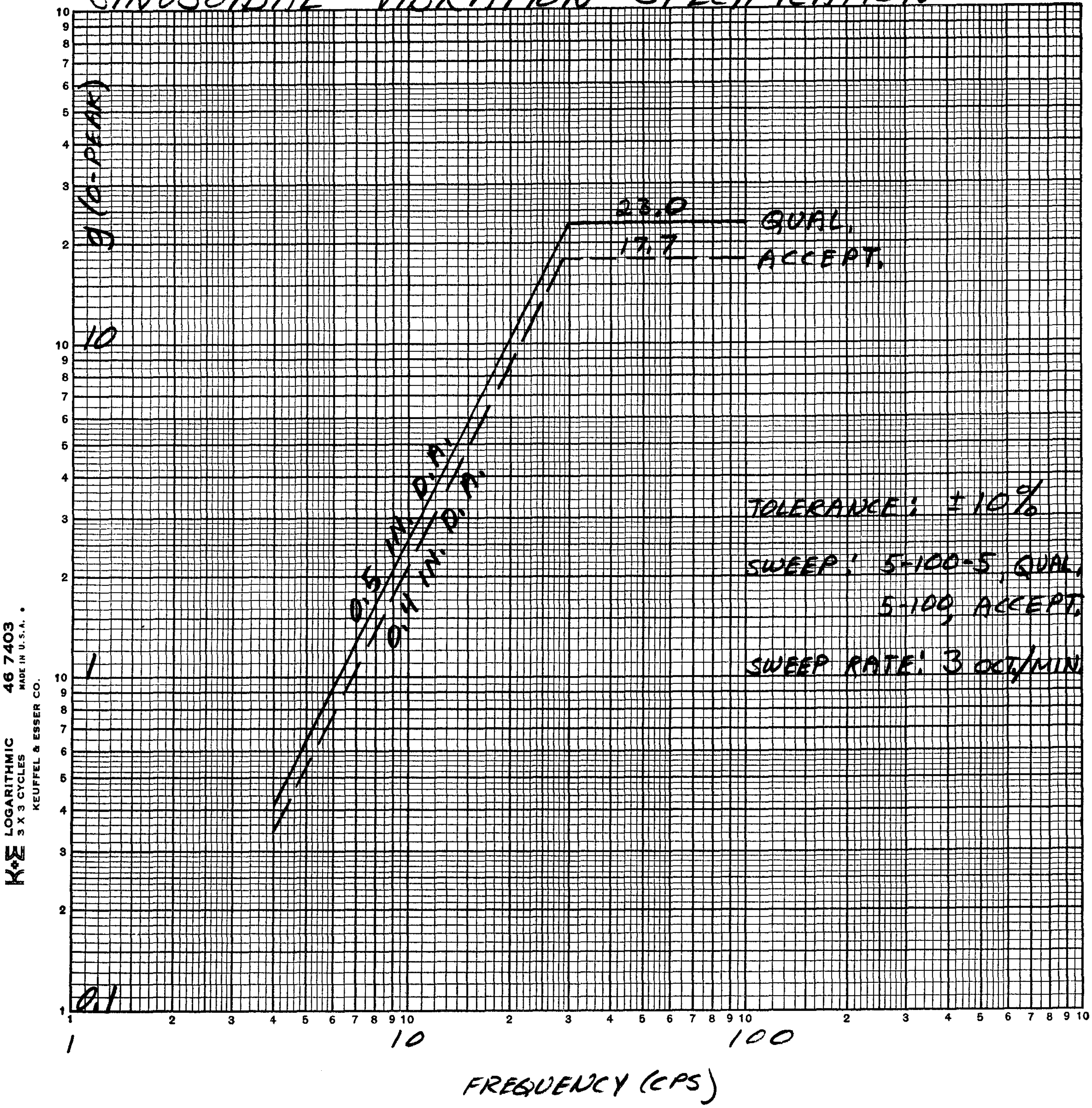

FIG. 7

RTG FUEL CASK
Z-AXIS
LAUNCH & BOOST
SINUSOIDAL VIBRATION SPECIFICATION

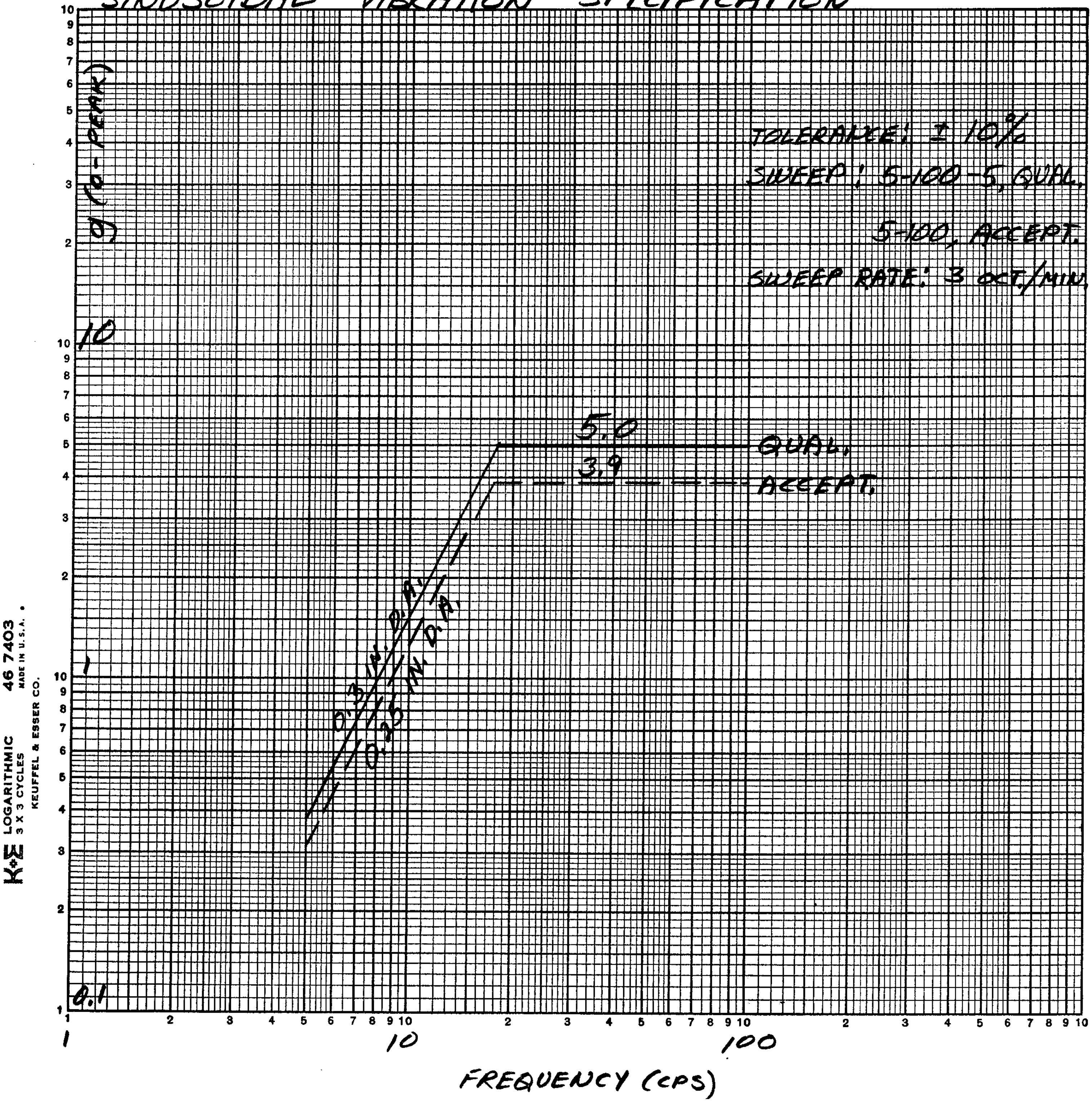

FIG. 8

RANDOM VIBRATION SPECIFICATION

CASK / X-AXIS / LAUNCH AND BOOST

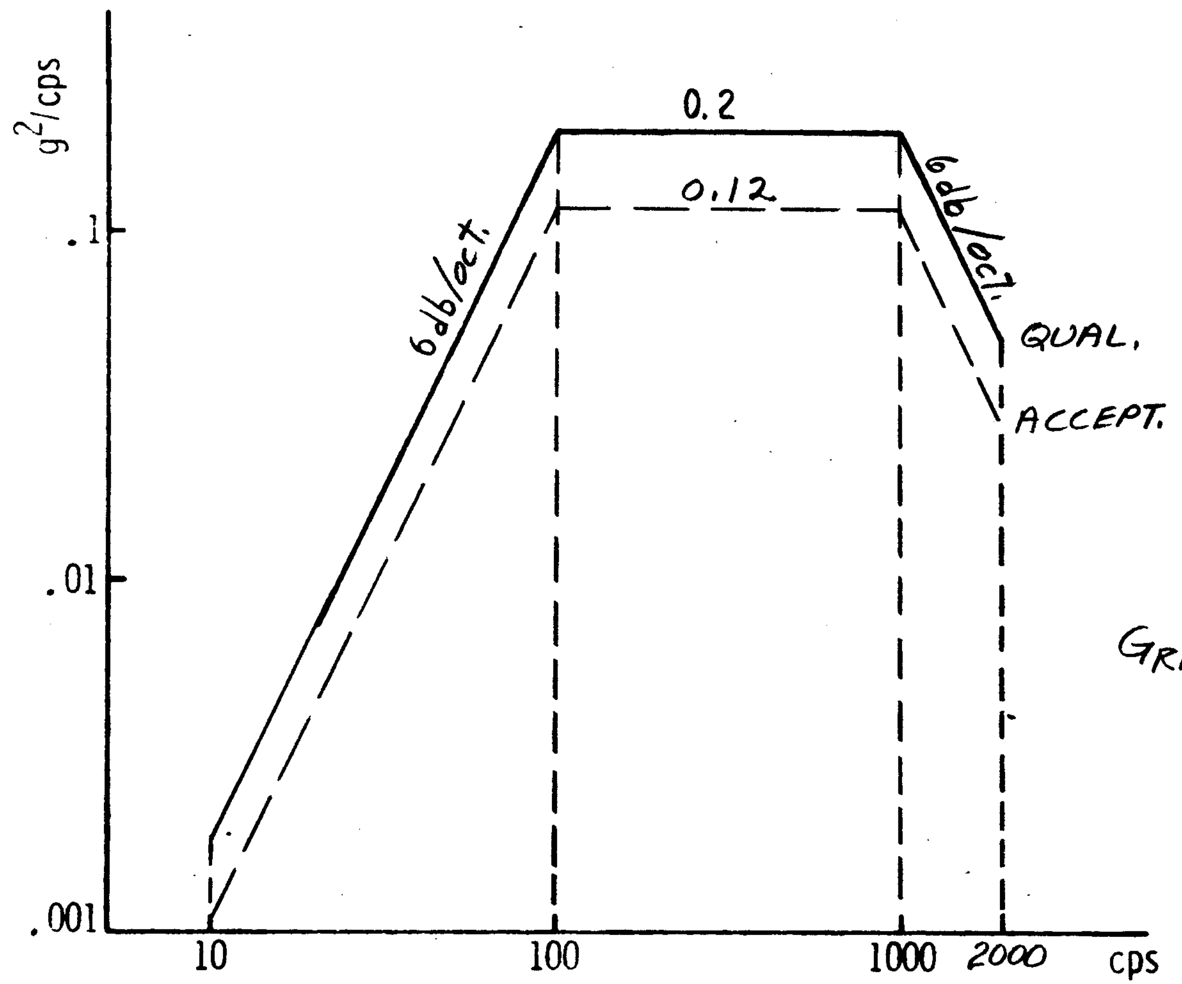

G_{RMS} = 16.9, QUAL.
= 13.0, ACCEPT.

FIG. 9

RANDOM VIBRATION SPECIFICATION

CASK / Y-AXIS / LAUNCH AND BOOST

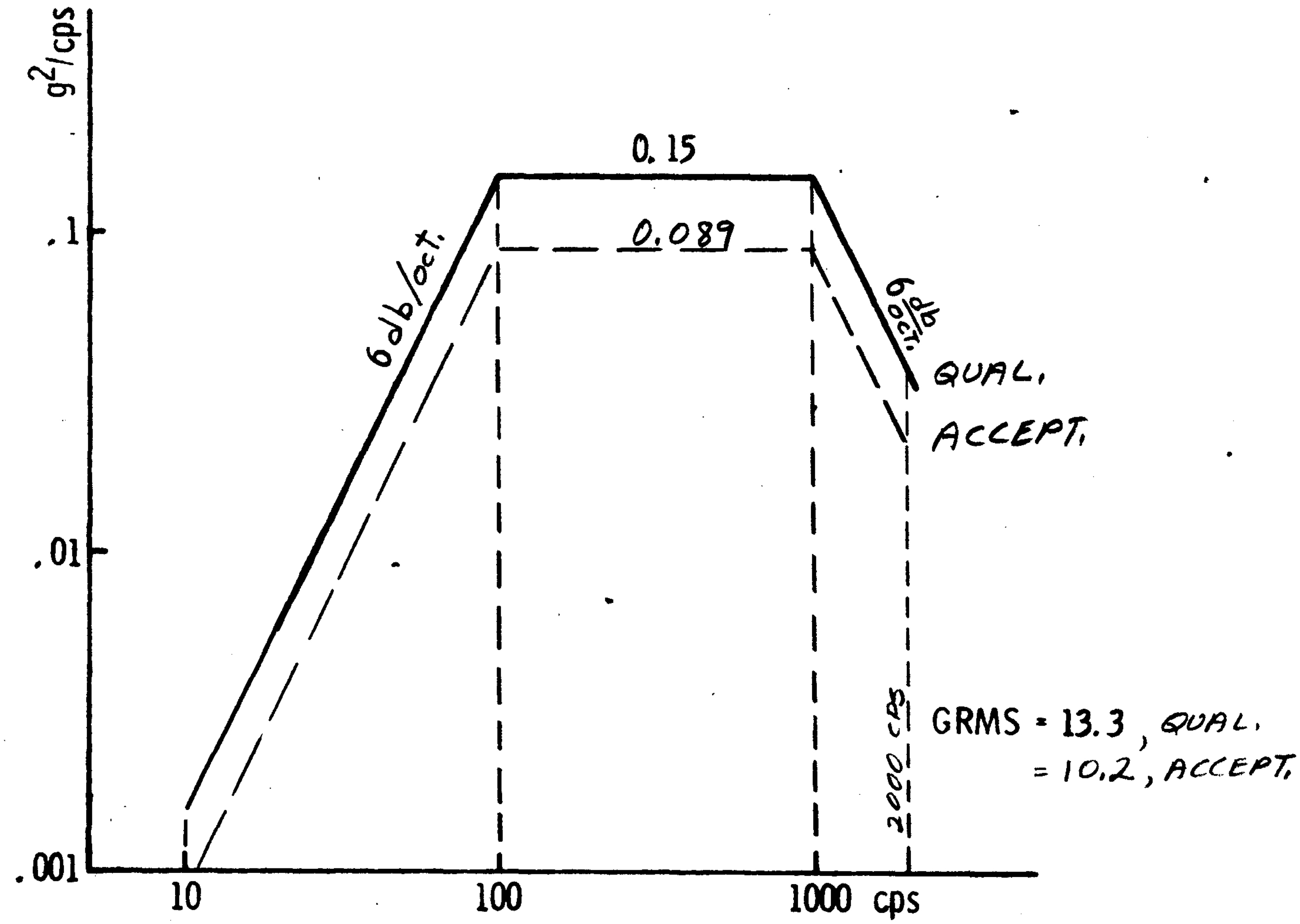

FIG. 10

RANDOM VIBRATION SPECIFICATION

CASK / Z-AXIS / LAUNCH AND BOOST

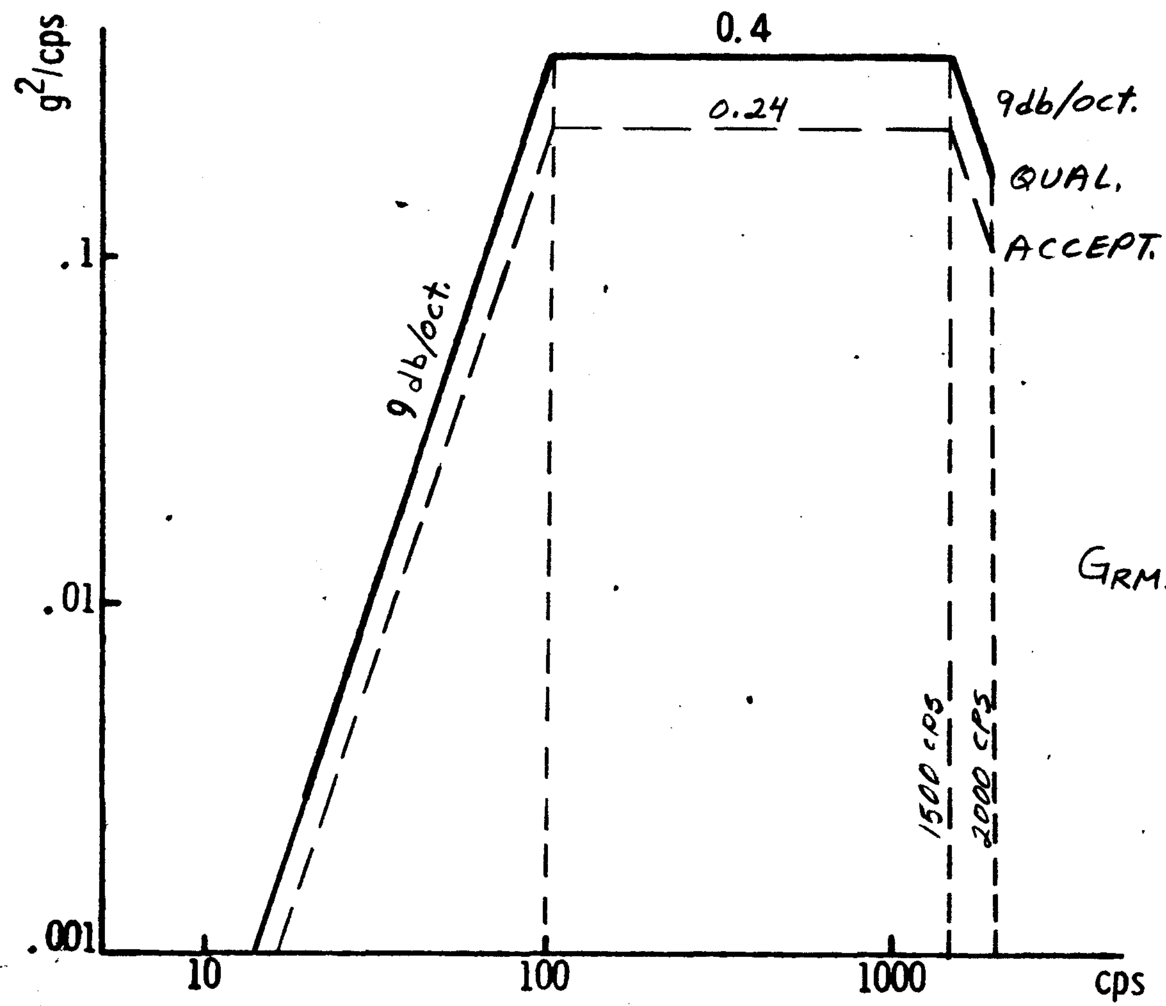

G_{RMS} = 26.3, QUAL.
= 20.2, ACCEPT.

FIG. 11

RTG FUEL CASK
X, Y, Z - AXES
LUNAR DESCENT
SINUSOIDAL VIBRATION SPECIFICATION

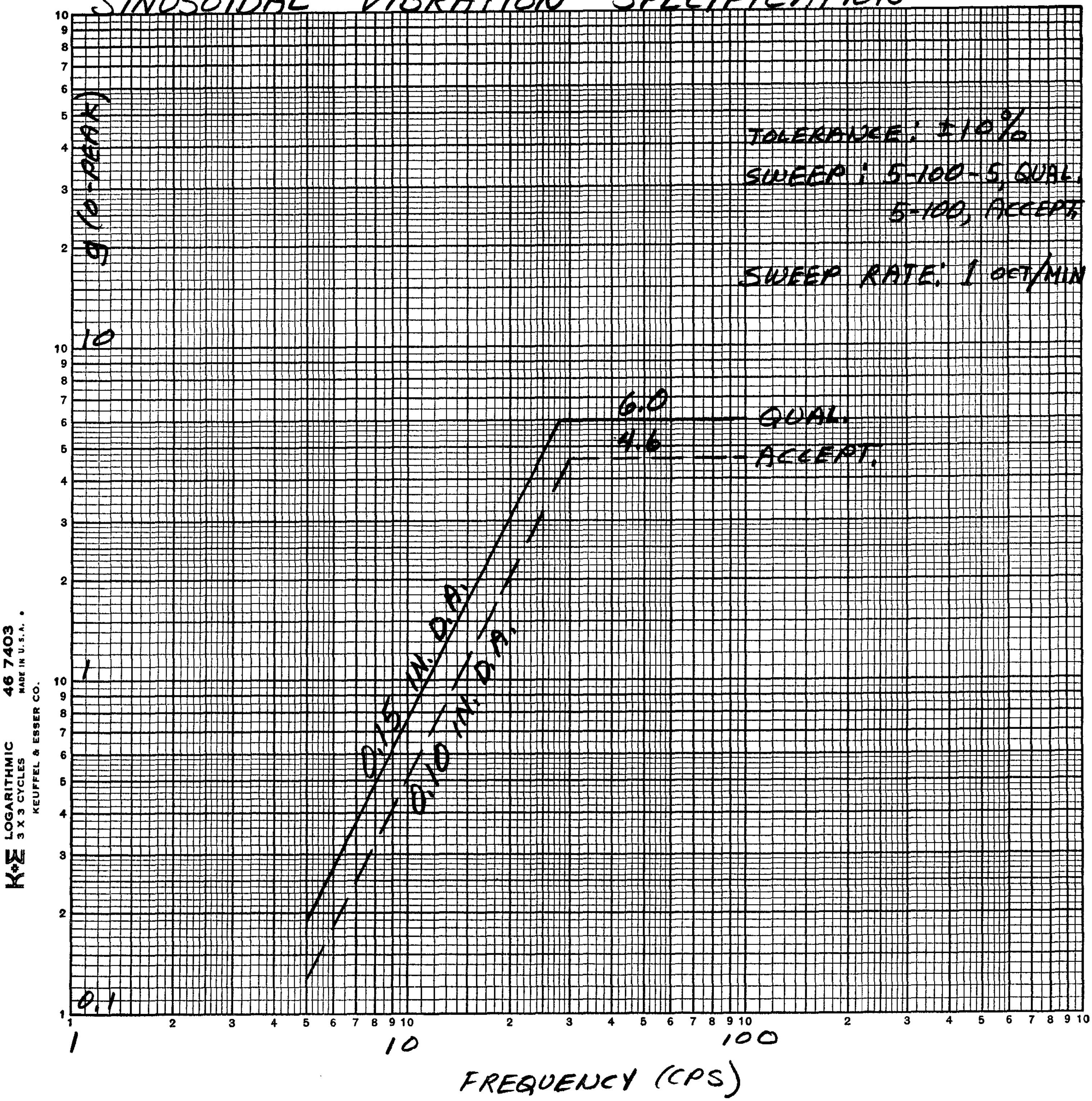

FIG. 12

RTG FUEL CASK
X & Y-AXES
LUNAR DESCENT
RANDOM VIBRATION SPECIFICATION

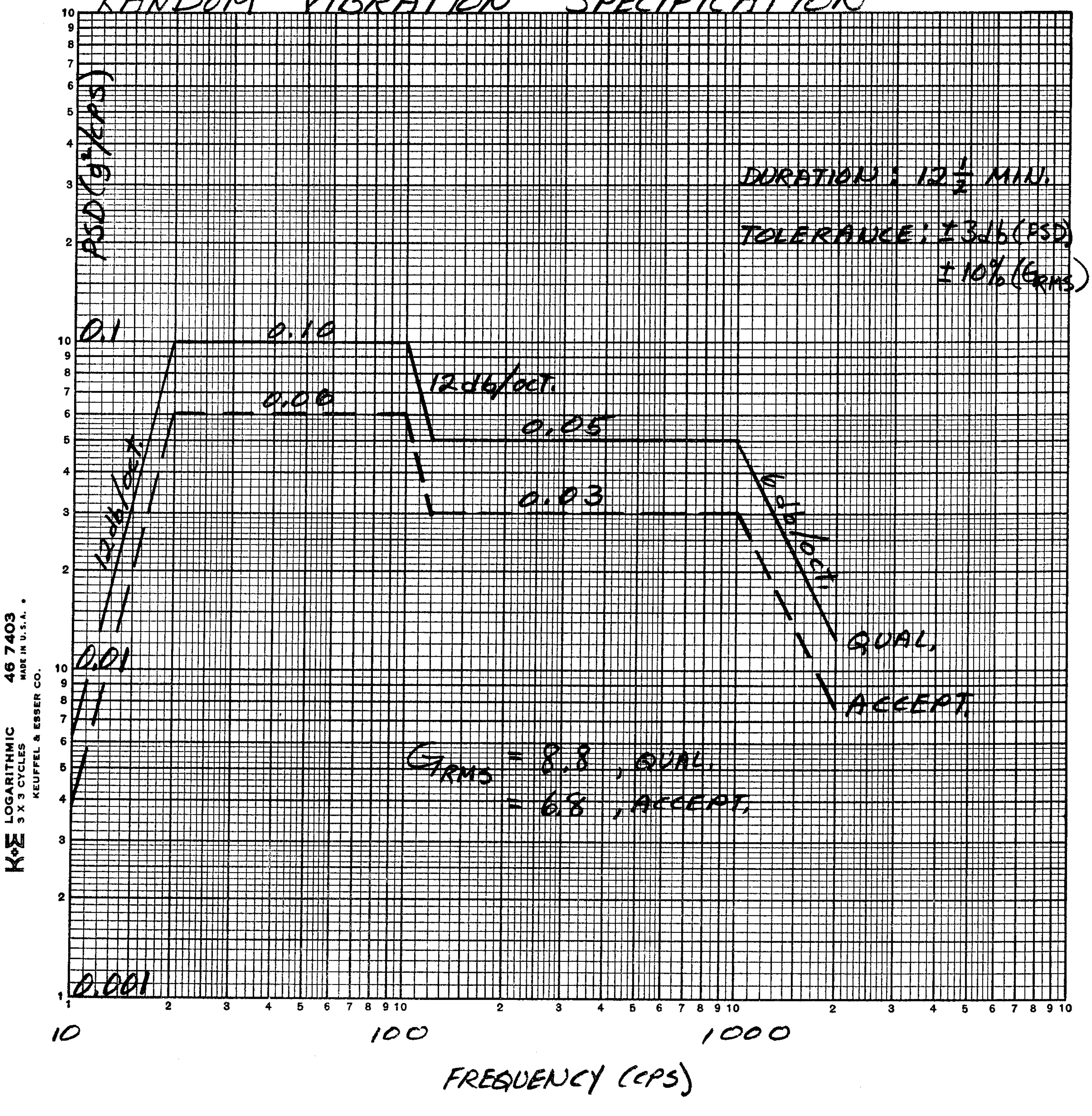

FIG. 13

RTG FUEL CASK
Z-AXIS
LUNAR DESCENT
RANDOM VIBRATION SPECIFICATION

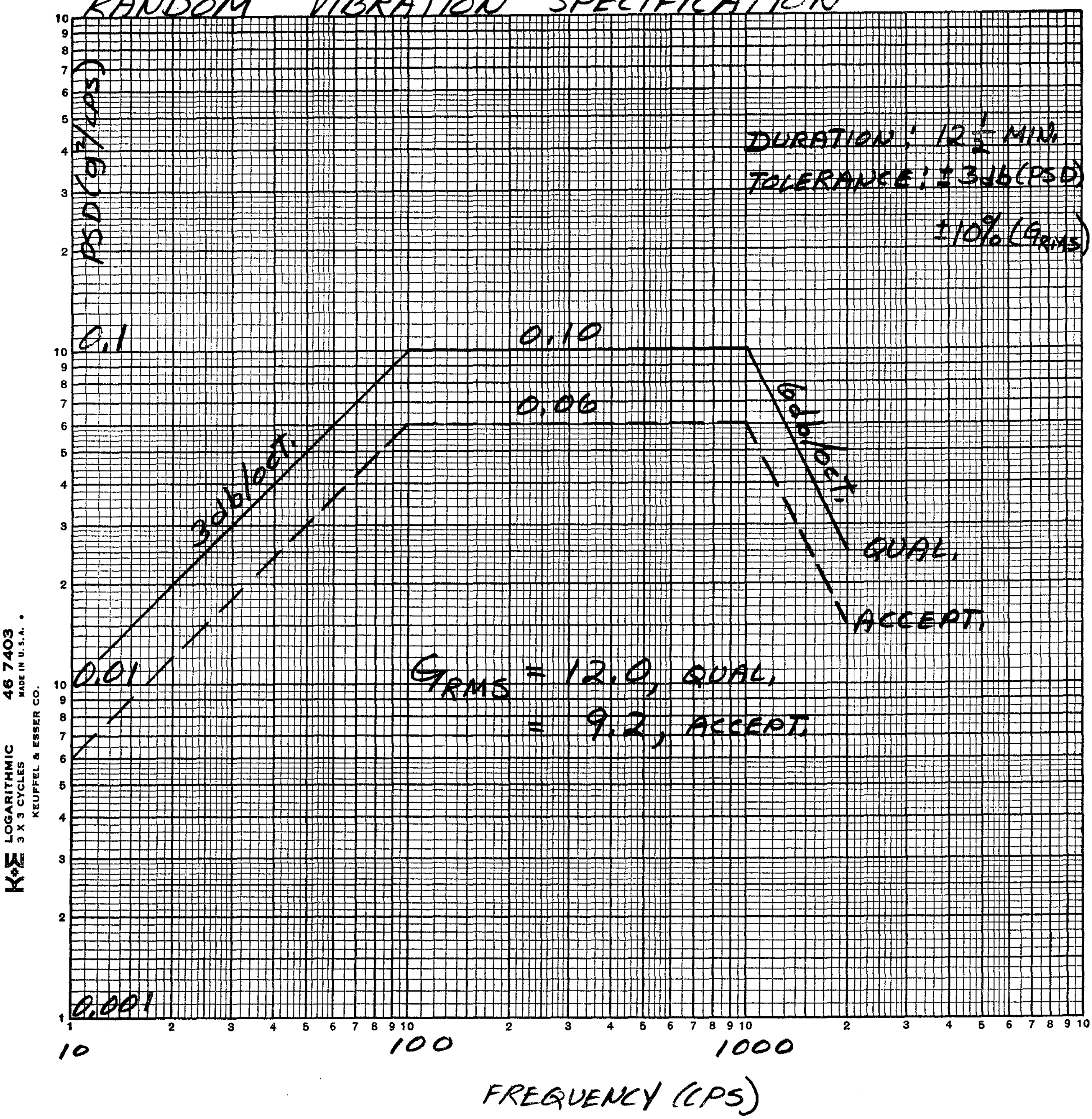

FIG. 14

ANALYSIS VS. TEST DATA

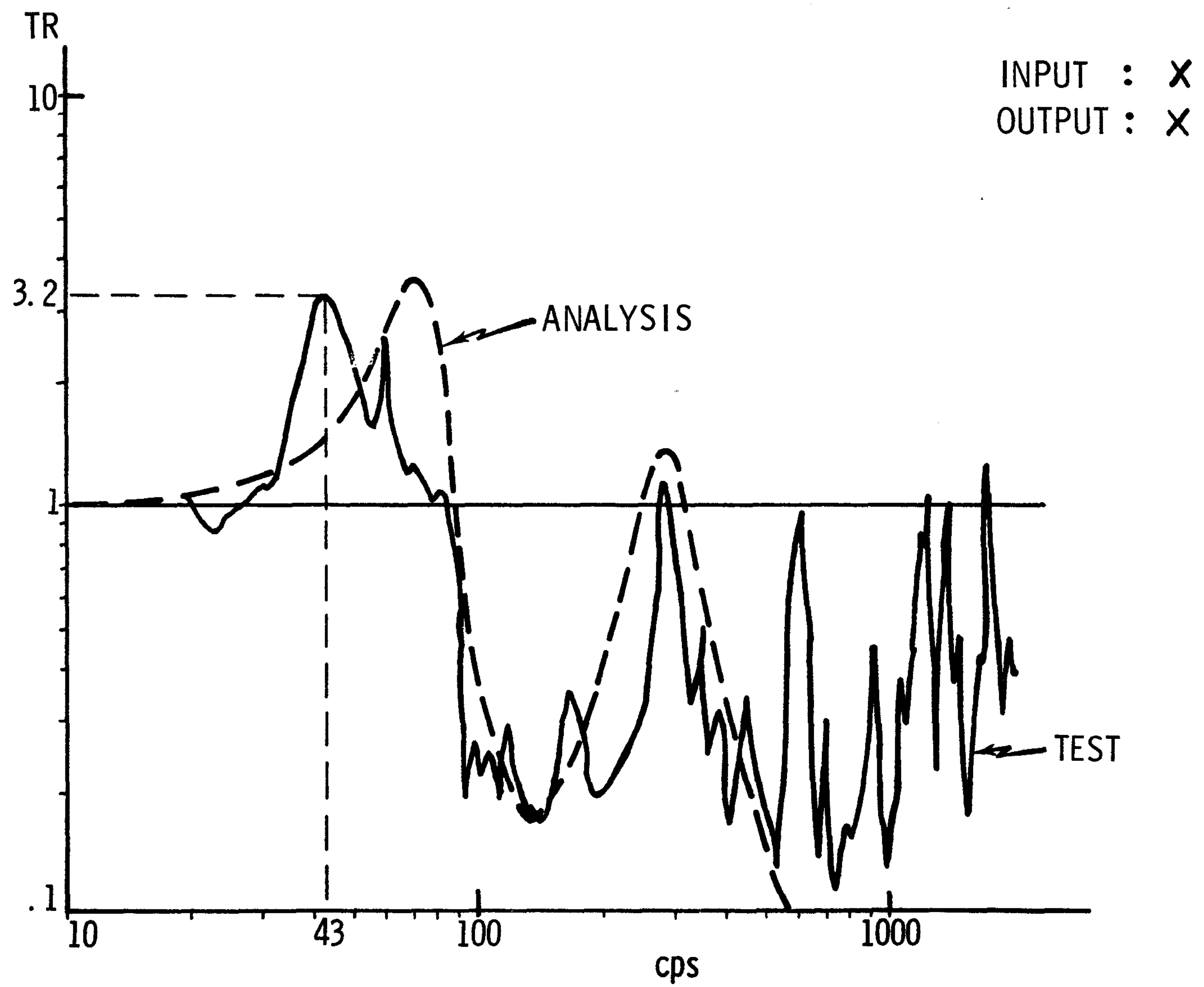

5607-5

FIG. 15

ANALYSIS VS. TEST DATA

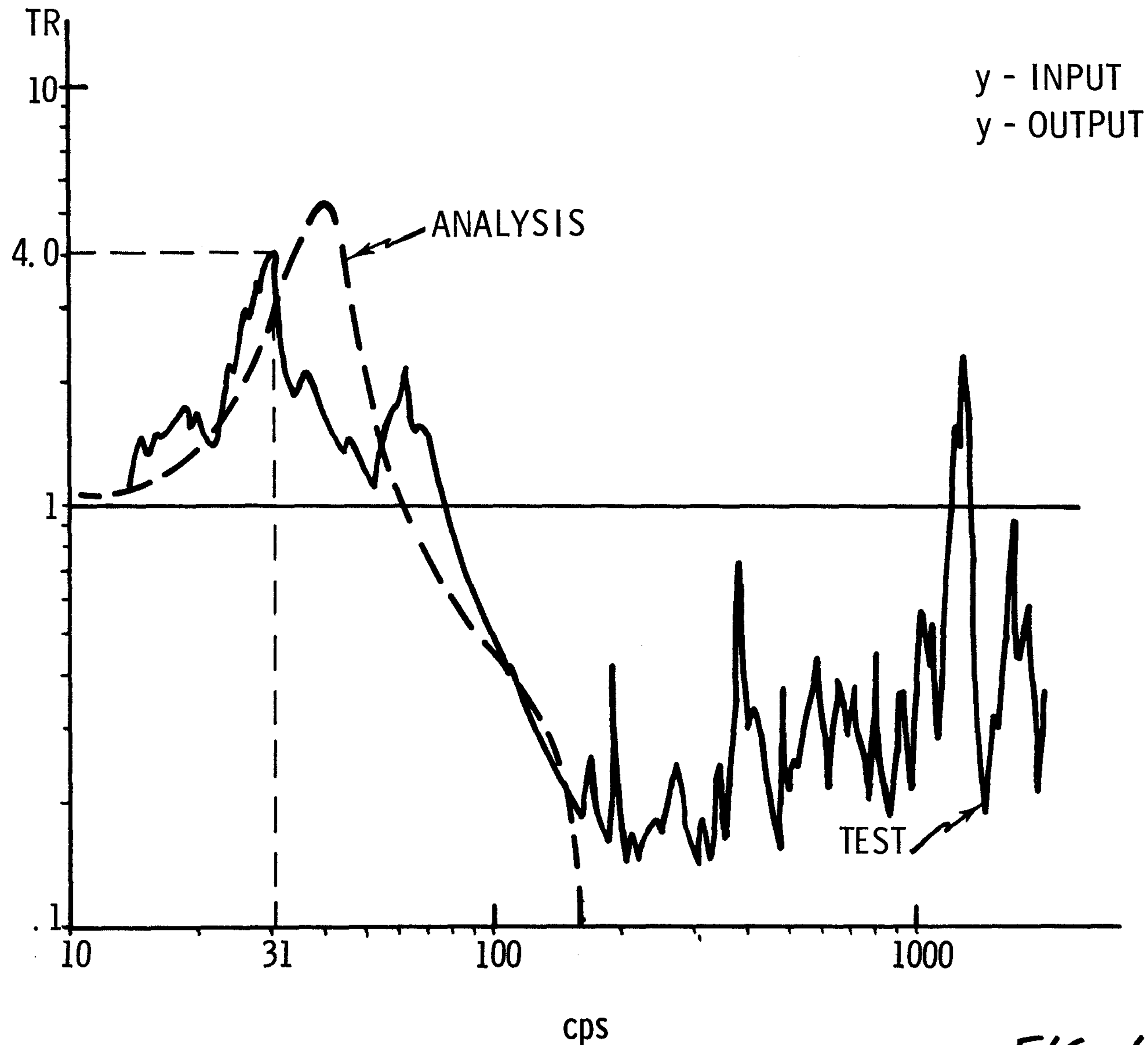

FIG. 16

5607-4

ANALYSIS VS. TEST DATA

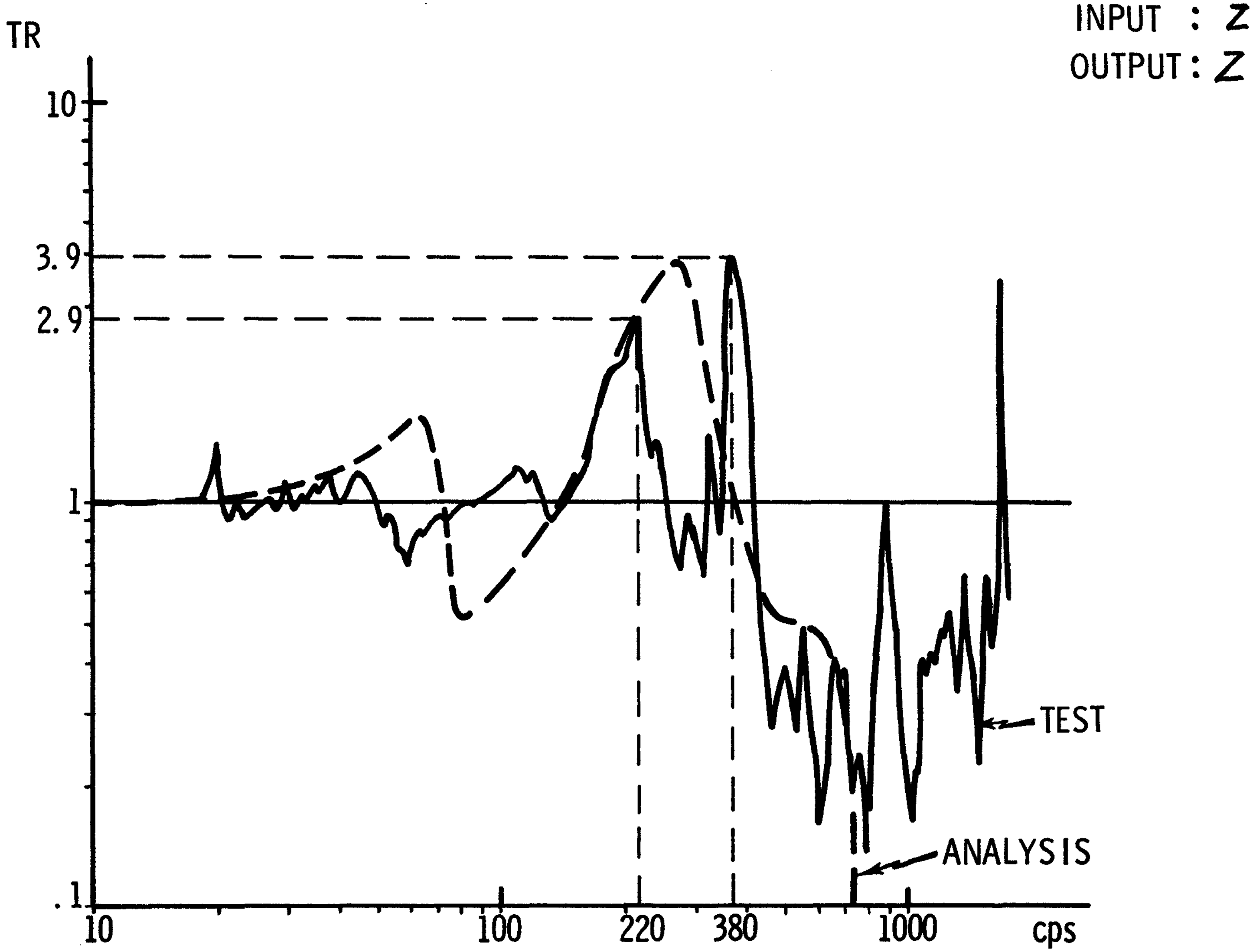

5607–3

FIG. 17

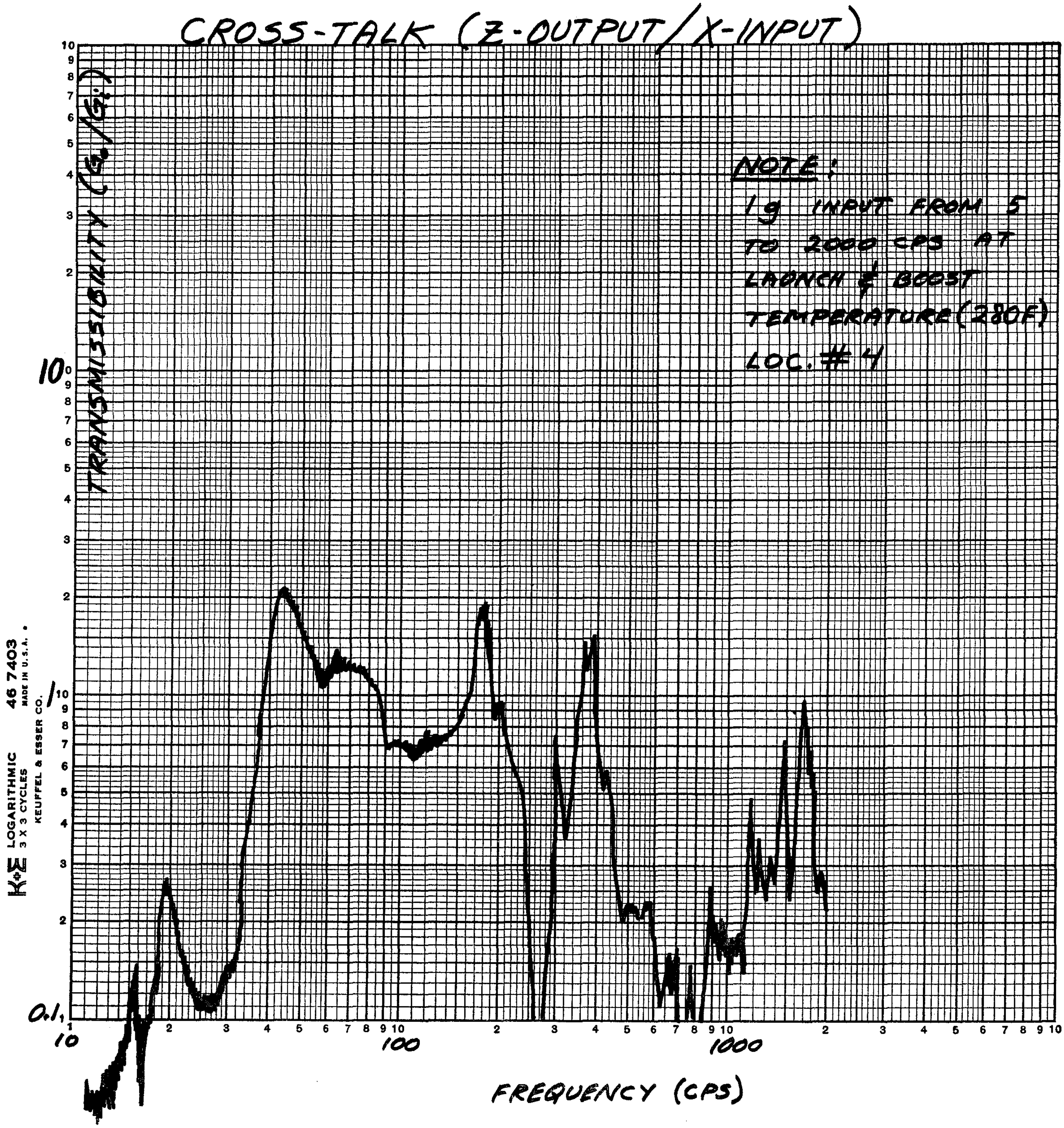
CROSS-TALK (Z-OUTPUT/X-INPUT)
TRANSMISSIBILITY (G₀/Gᵢ)
NOTE:
1g INPUT FROM 5 TO 2000 CPS AT LAUNCH & BOOST TEMPERATURE (280F)
LOC. #4
FREQUENCY (CPS)
0.1
1
10
10
100
1000

FIG. 18

1G SWEEP LAUNCH AND BOOST

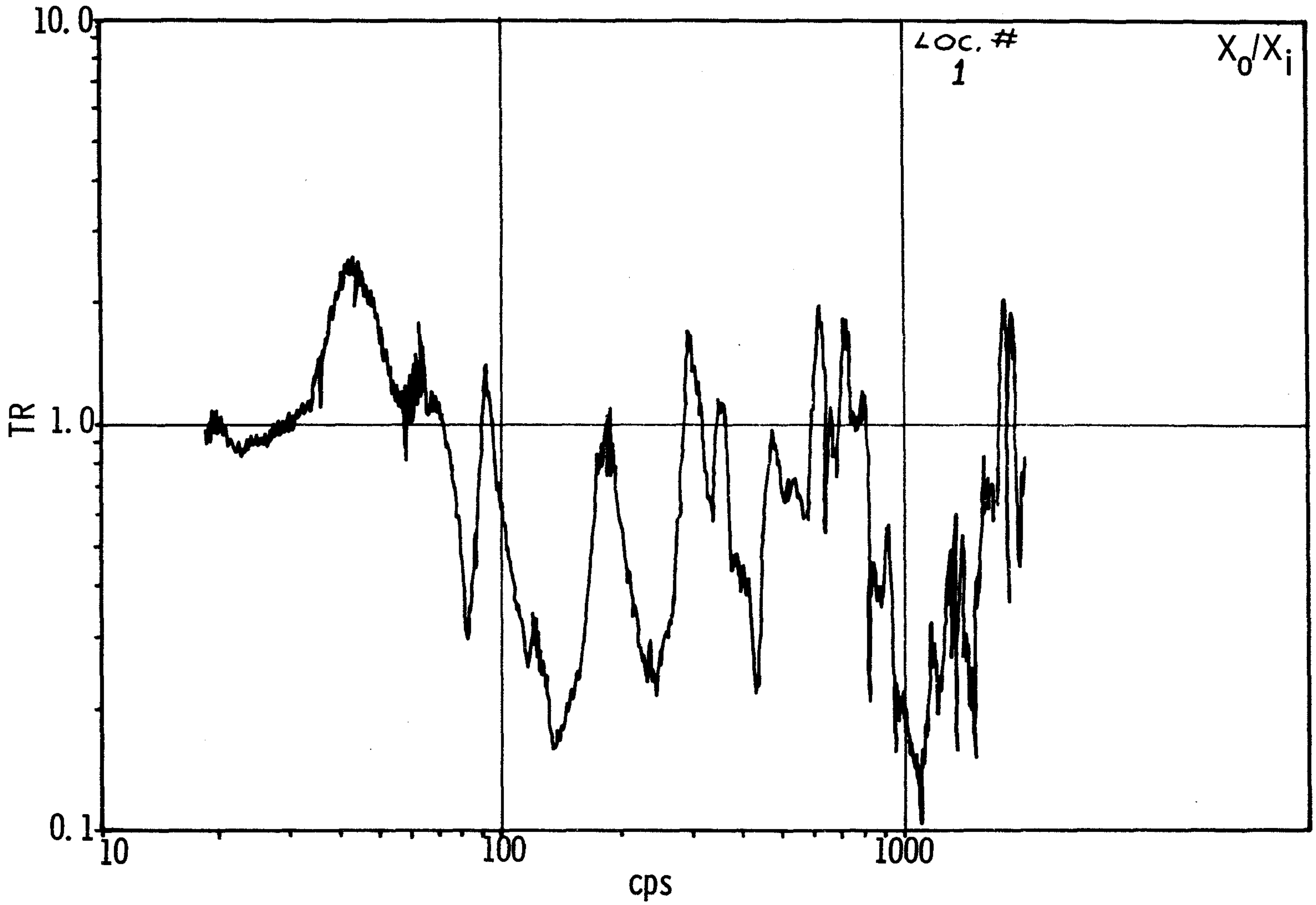

5607-8

FIG. 19

1G SWEEP LAUNCH AND BOOST

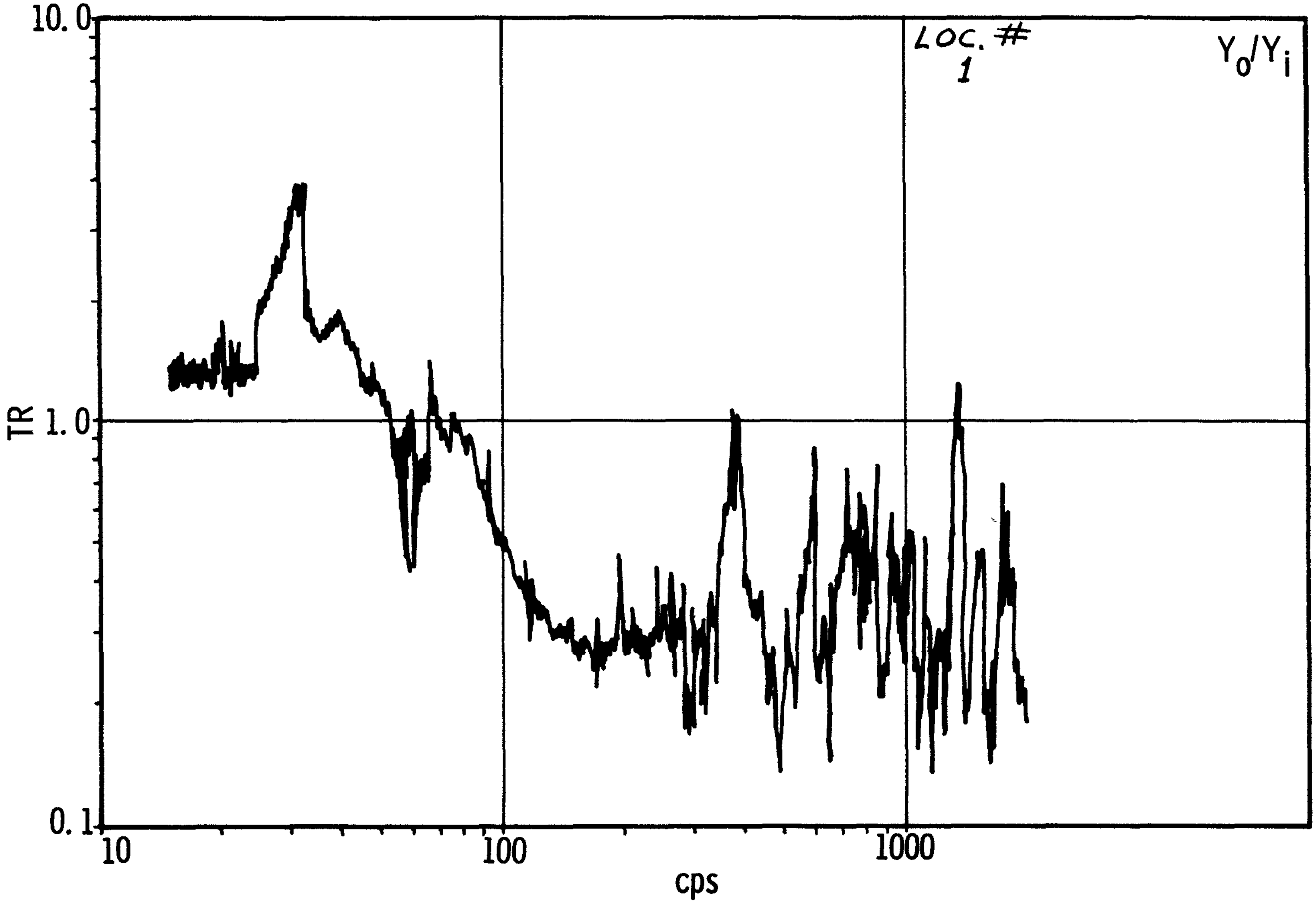

FIG. 20

5607–10

1G SWEEP LAUNCH AND BOOST

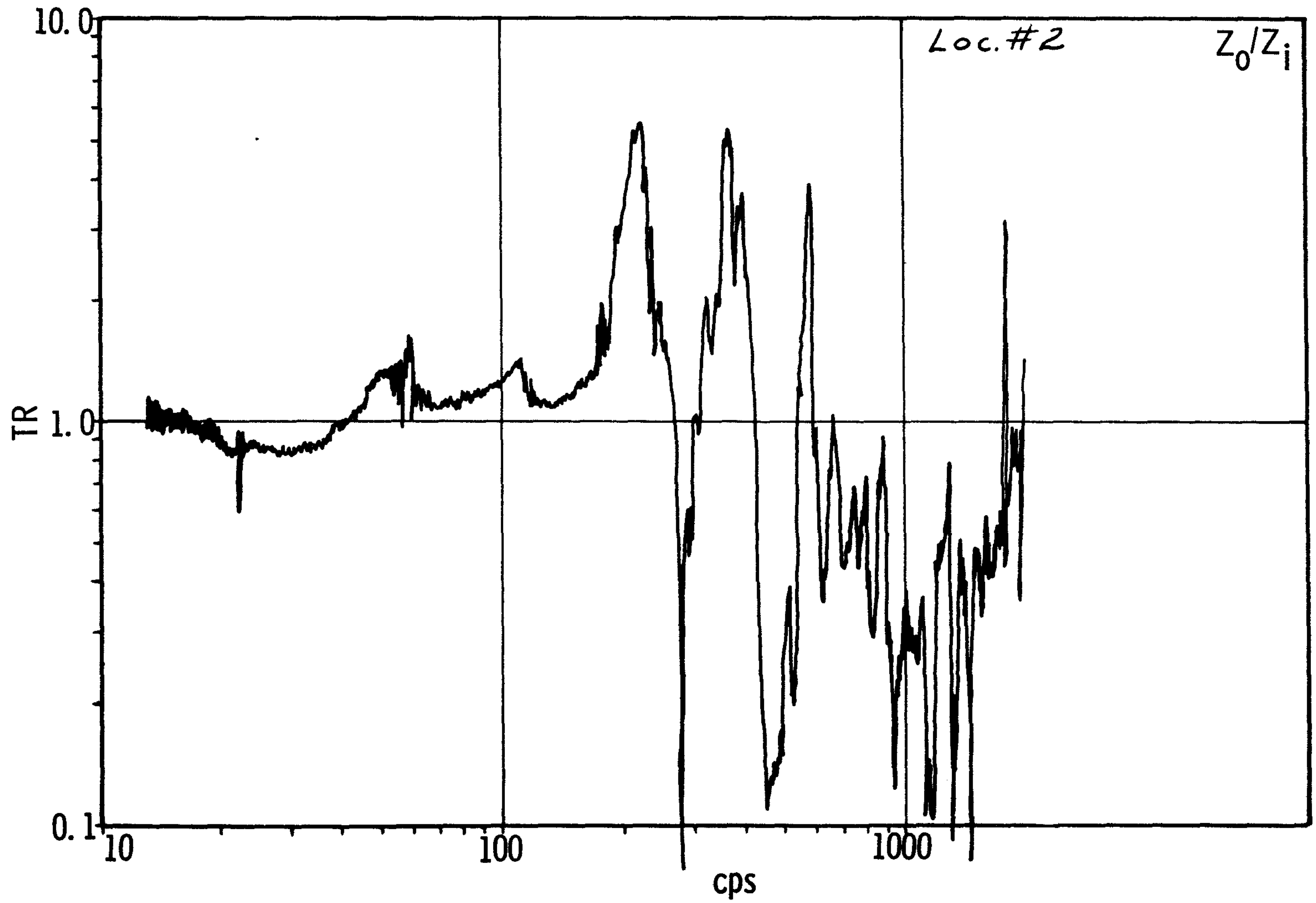

FIG. 21

5607–12

1G SWEEP LUNAR DESCENT

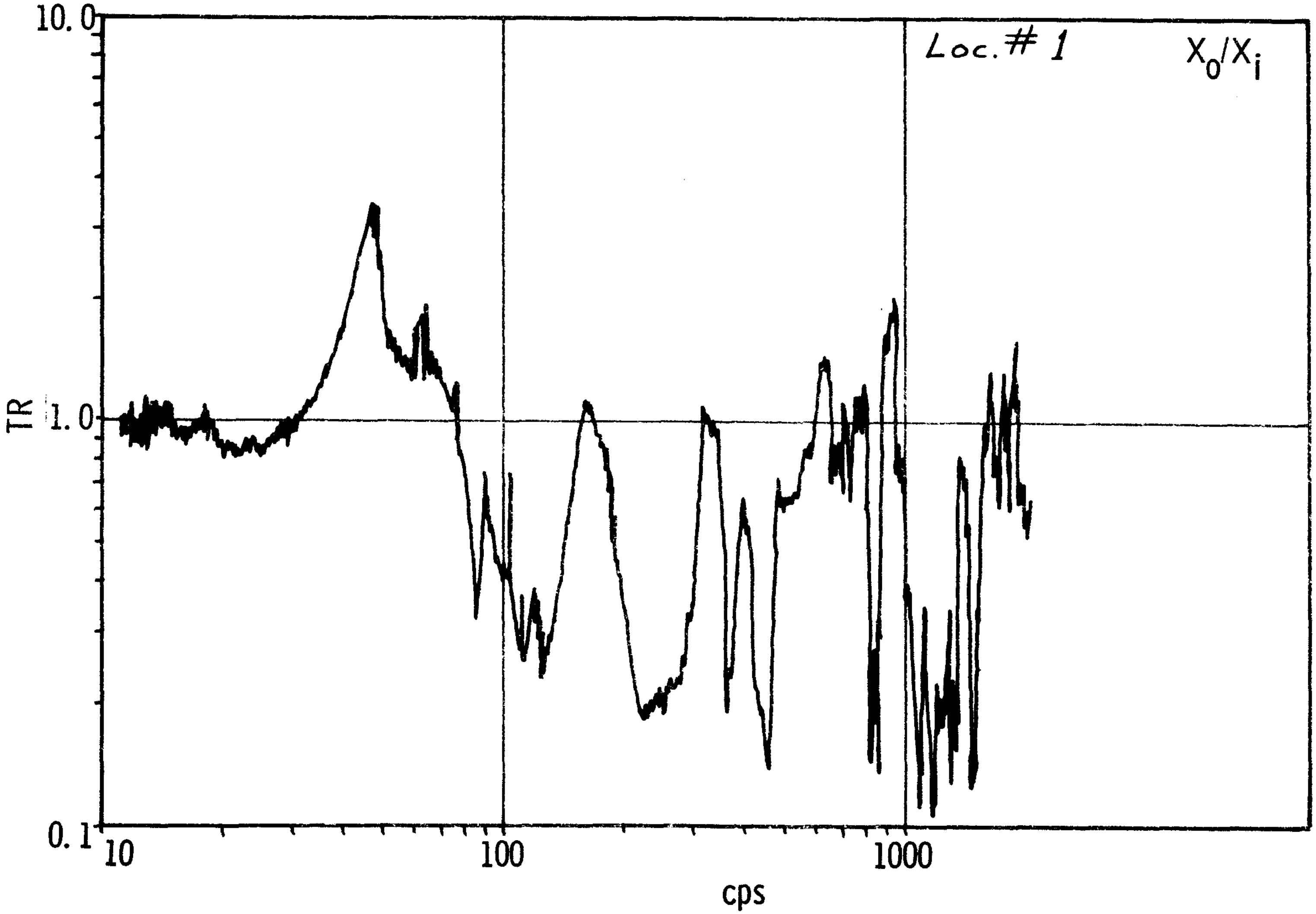

5607-9

FIG. 22

1G SWEEP LUNAR DESCENT

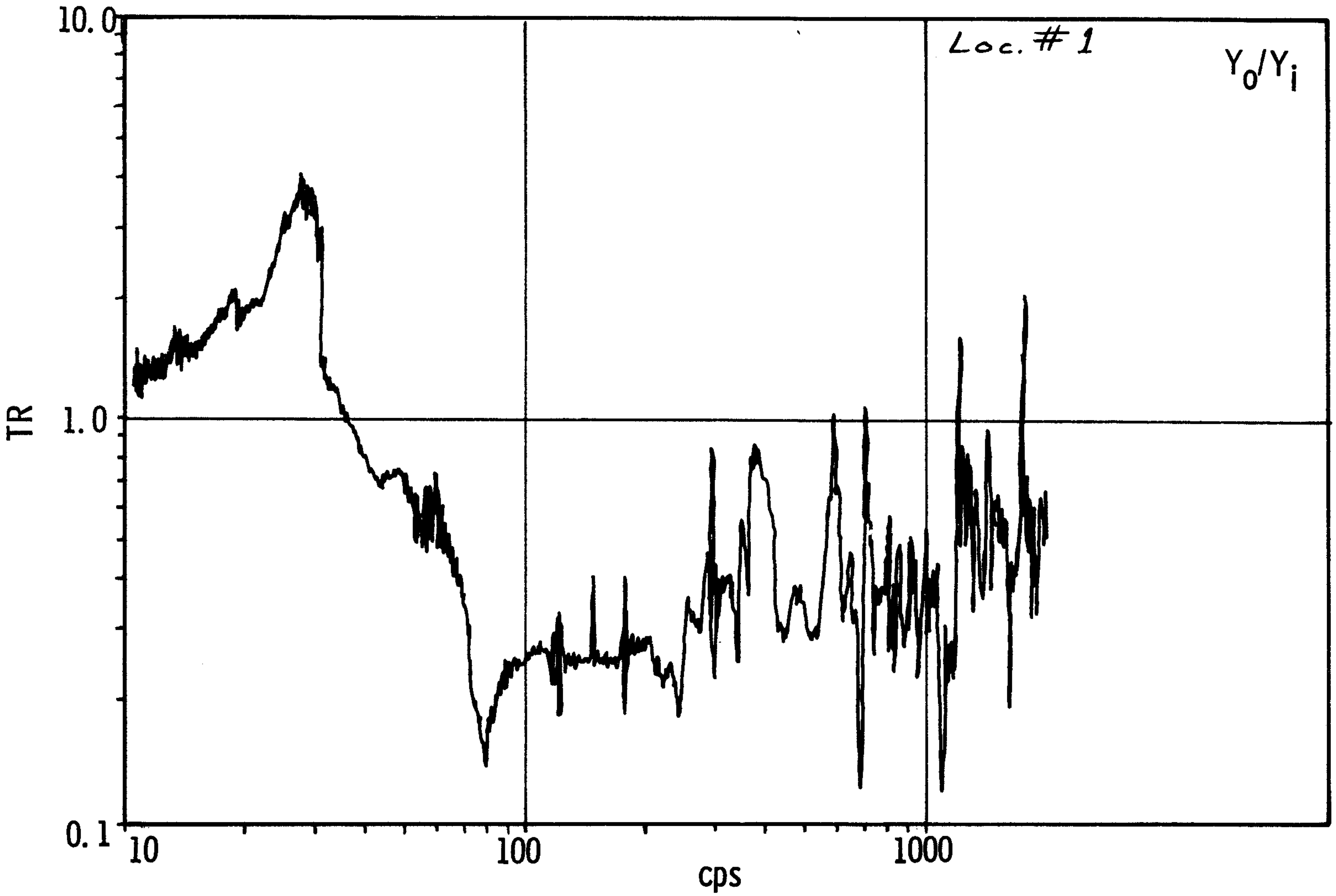

5607-11

FIG. 23

1G SWEEP LUNAR DESCENT

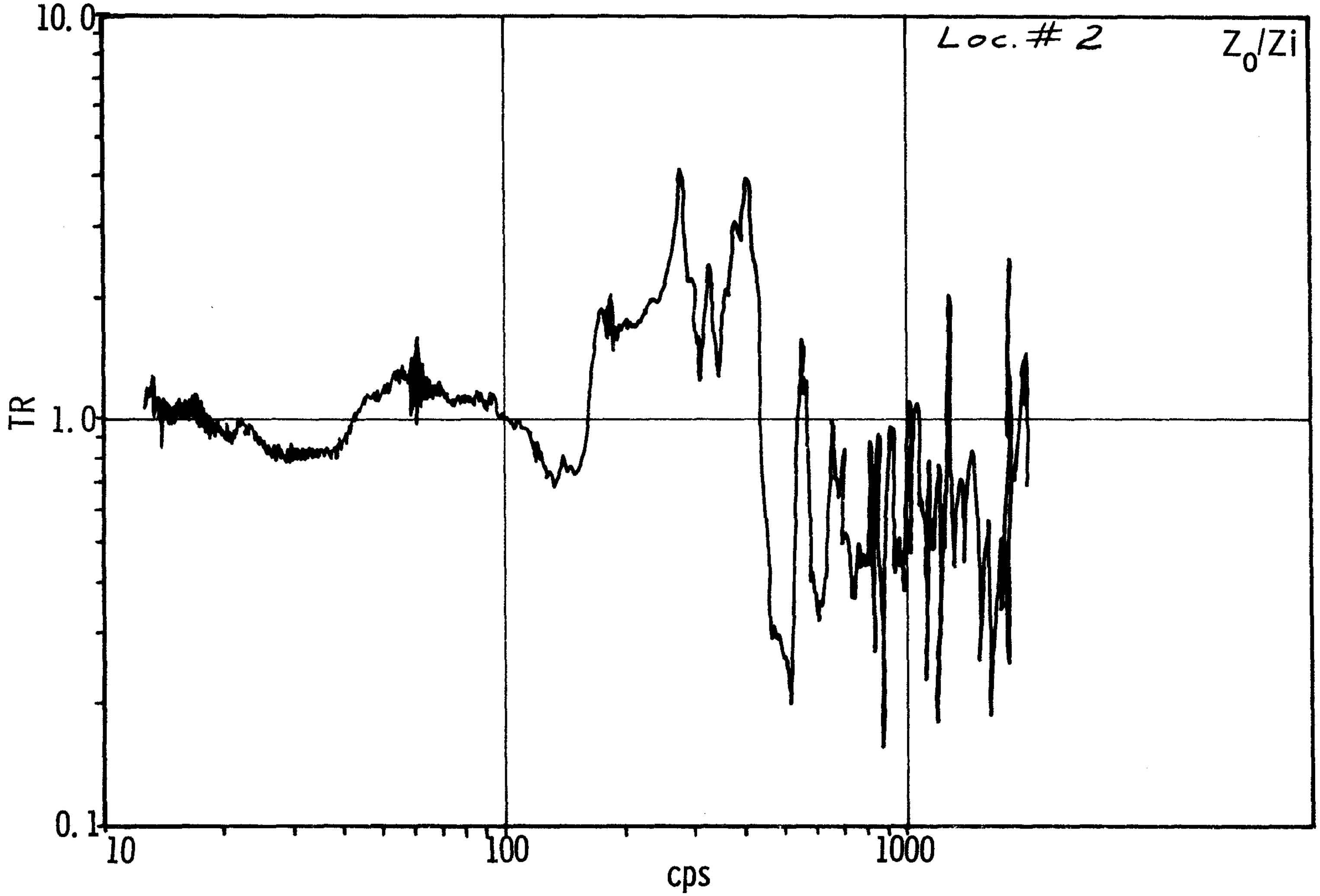

FIG. 24

5607–16

LAUNCH AND BOOST SINE TRANSMISSIBILITY -X AXIS

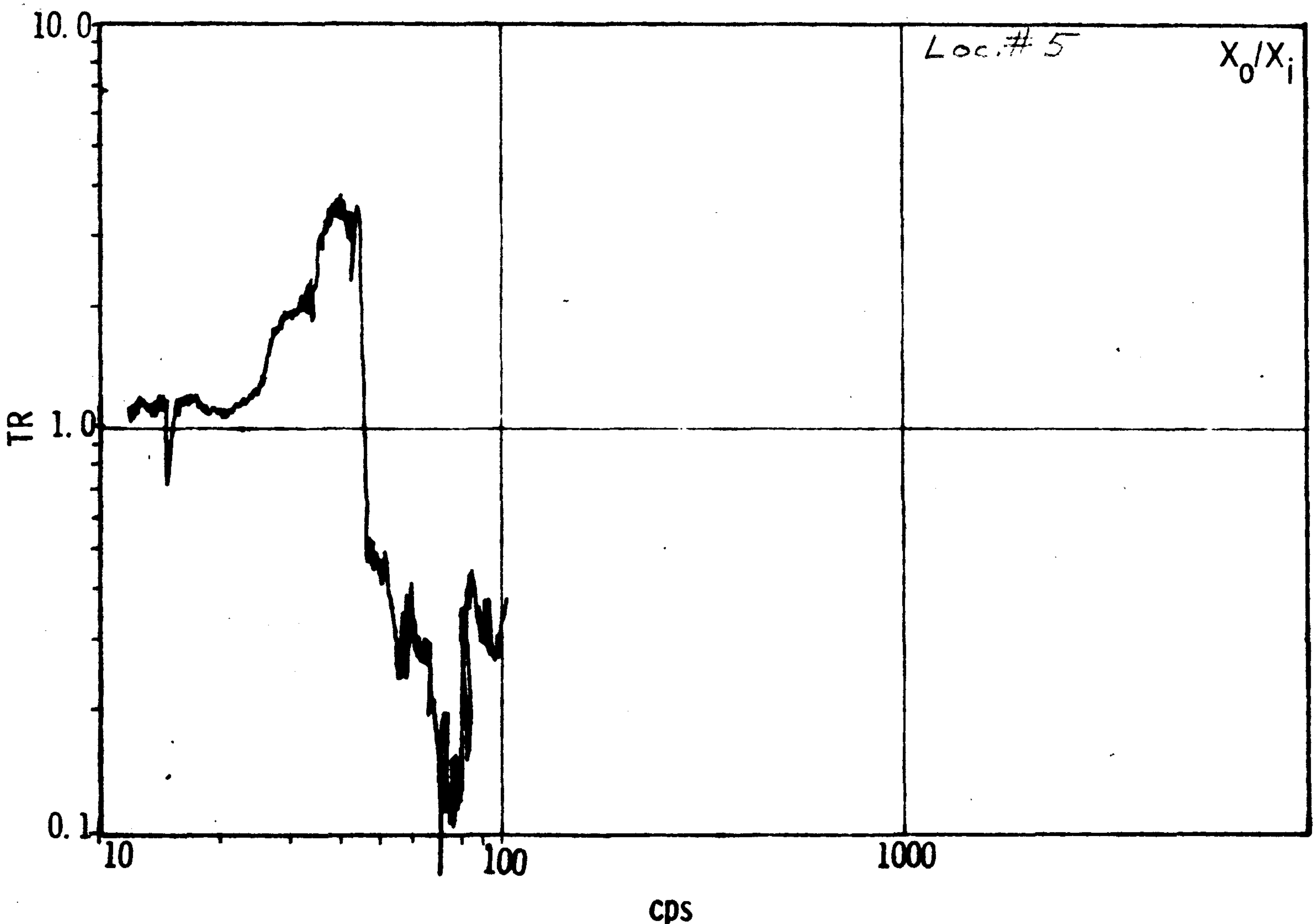

FIG. 25

TRANSMISSIBILITY - Y AXIS

LAUNCH AND BOOST SINE

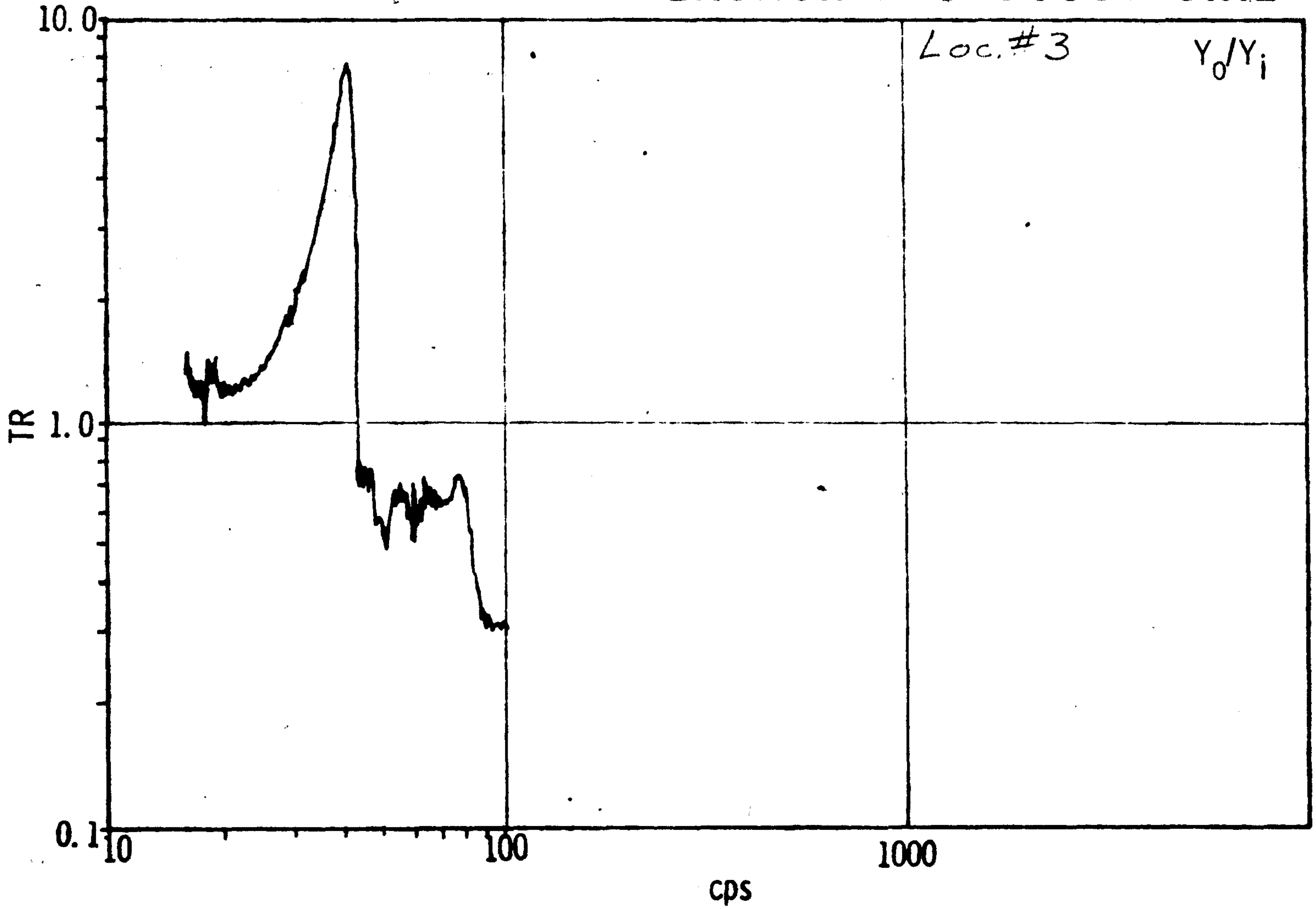

FIG. 26

LAUNCH AND BOOST SINE
TRANSMISSIBILITY - Z AXIS

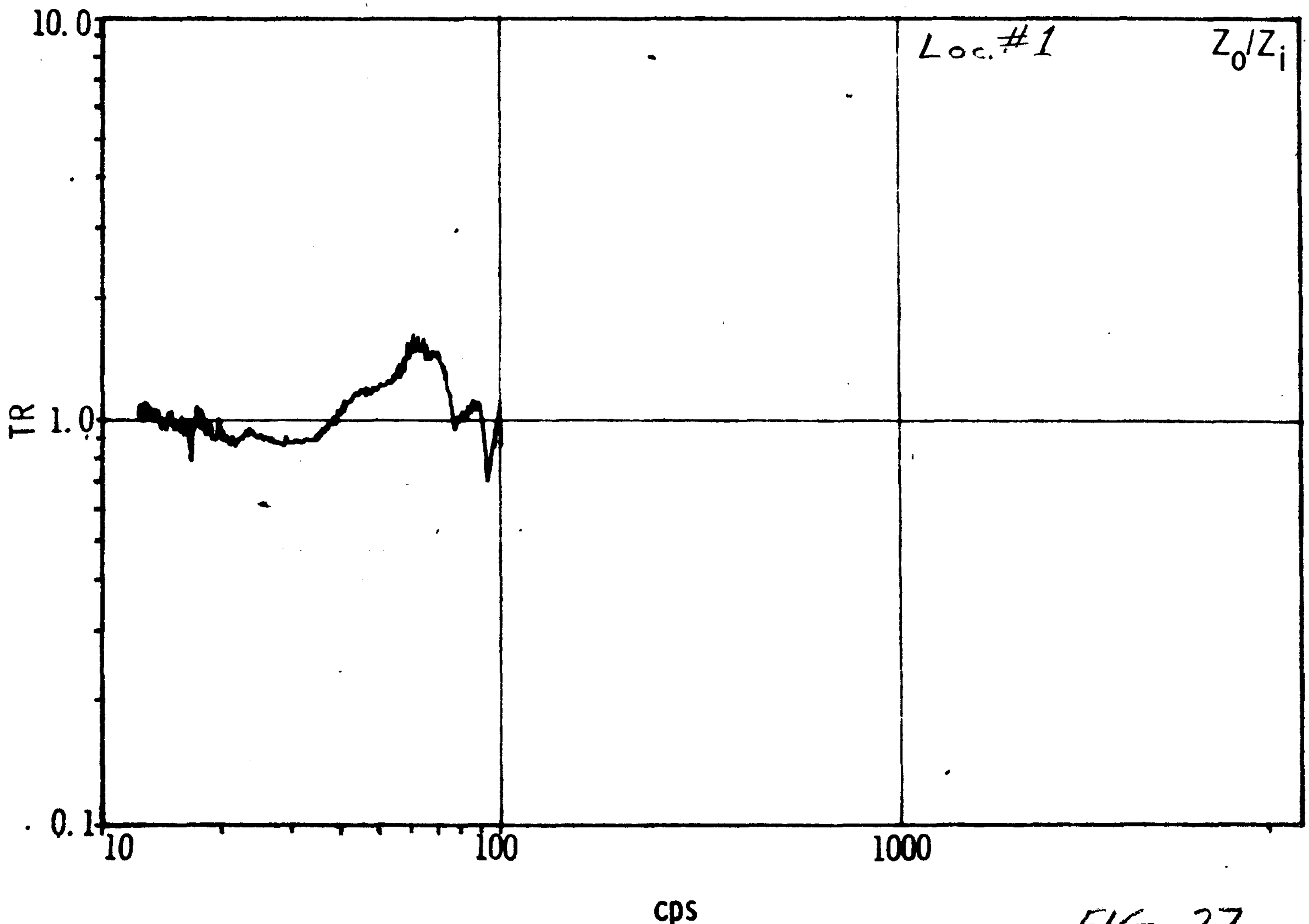

FIG. 27